

Low Fatigue Designs and Deep Learning-based Classification for Motion Visual Evoked Potentials

Raika Karimi

A Thesis

in

The Department

of

Electrical and Computer Engineering

Presented in Partial Fulfillment of the Requirements

for the Degree of

Master of Applied Science (Electrical and Computer Engineering) at

Concordia University

Montréal, Québec, Canada

December 2020

© Raika Karimi , 2021

**CONCORDIA UNIVERSITY
SCHOOL OF GRADUATE STUDIES**

This is to certify that the thesis prepared

By: Raika Karimi

Entitled: Low Fatigue Designs and Deep Learning-based Classification for Motion Visual Evoked Potentials

and submitted in partial fulfillment of the requirements for the degree of

Master of Applied Science (Electrical and Computer Engineering)

complies with the regulations of this University and meets the accepted standards with respect to originality and quality.

Signed by the final examining committee:

_____	Chair
Dr. H. Benali	
_____	External Examiner
Dr. Y. Zeng (CIISE)	
_____	Internal Examiner
Dr. H. Benali	
_____	Co-Supervisor
Dr. A. Asif	
_____	Co-Supervisor
Dr. A. Mohammadi (CIISE)	

Approved by: _____
Dr. Y.R. Shayan, Chair
Department of Electrical and Computer Engineering

_____ 20____

Dr. Mourad Debbabi, Interim Dean,
Gina Cody School of Engineering and
Computer Science

Abstract

Low Fatigue Designs and Deep Learning-based Classification for Motion Visual Evoked Potentials

Raika Karimi

Recent advancements in Electroencephalography (EEG) sensor technologies, Signal Processing (SP), and Machine Learning (ML) algorithms have paved the way for further evolution of Brain Computer Interfaces (BCI) in several practical applications ranging from rehabilitation systems to smart consumer technologies. In particular, this thesis research is motivated by potentials of BCI platforms to provide comfortable means for individuals with communication disabilities to interact with the outer world. When it comes to SP/ML models for BCI systems, there has been a surge of interest on Visual Evoked Potentials (VEPs). Recently, Steady-state visual evoked potential (SSVEP) has become popular due to their fast and reliable performance, and strong provocation of visual brain signals. Despite the popularity of SSVEPs, their utilization for practical applications especially for assistive technologies is challenging due to eye fatigue and risk of induced epileptic seizure. In this regard, the key issue of conventional light-flashing techniques has been addressed by development of flicker-free Steady-State motion Visual Evoked Potential (SSmVEP). Such benefits, however, come with the price of having less accuracy and less Information Transfer Rate (ITR). In this regard, the thesis focuses on improving the following three main components: (i) *Stimulation paradigm*; (ii) *Frequency modulation*, and; (iii) *Target classification* in SSmVEP-based BCIs. With regard to the first component, novel SSmVEP paradigms with low luminance contrast and oscillating expansion and contraction motions are designed, and integrated within a BCI system. Through experimental evaluations, high detection accuracies are achieved for our proposed paradigms leading to less visual tiredness in comparison to conventional SSVEPs. Concerning the second component, an efficient modulation mechanism is proposed without using resources such

as trial time, phase, and/or number of targets to enhance the ITR. The proposed design is based on the intuitively pleasing idea of integrating more than one motion within a single SSmVEP target stimuli, simultaneously. To elicit SSmVEP, we designed a novel and innovative dual frequency aggregated modulation paradigm, referred to as the Dual Frequency Aggregated steady-state motion Visual Evoked Potential (DF-SSmVEP). The proposed DF-SSmVEP is evaluated based on a real EEG dataset and the results corroborate its superiority. With respect to the third component, it is expected that incorporation of human brain's nonlinear dynamics and characteristics of the designed videos within our EEG signal classifier lead to a comprehensive model resulting in better noise removal. To this end, a deep learning-based classification model is proposed, referred to as the Deep Video Canonical Correlation Analysis (DvCCA), that extracts features of the SSmVEPs directly from the videos of stimuli. The proposed DvCCA is evaluated based on a real EEG dataset and the results corroborate its superiority against recently proposed state-of-the-art Convolutional Neural Network-based models.

Acknowledgments

First and foremost, praises and thanks to my leader, supporter, and role model in my life, Prof. Arash Mohammadi, for candidly helping me to complete the research successfully.

I would like to express my deep and sincere gratitude to my research supervisor, Prof. Arash Mohammadi, whose extensive knowledge, motivation, and backing cause my research project to be done perfectly. I would also like to thank him for his friendship, empathy, kindness. I cannot forget the nights when he stayed awake to help me to prepare my papers. Without the supervision of him, I could not overcome the challenges I faced during my academic as well as personal life.

I want to send my deep gratitude to my supervisor Prof. Amir Asif, whose guidance, support, and awareness made this project possible. His dynamism, vision, sincerity, and motivation have deeply inspired me. It was a great privilege and honor to work and study under his supervision.

Besides my supervisors, I would like to thank Prof. Habib Benali, who is indeed a hero in neuroscience, for contributing to some parts of the project. I have learned a lot from him and his delicate advices. I am very much thankful to Laura Isabel Rosero for designing the paradigms used in my research. I could not have performed experiments without her endeavor and the generous endowment of intelligence.

I am extending my heartfelt thanks to my parents for their love, caring, and sacrifices to educate and prepare me for my future. I send my endless appreciation to my great parents, who are the most important assets in my life.

I thank my best friend, Arash, who accompany me every moment of the past two years.

And finally, I thank my lab mates for sharing their knowledge and support with me. It was great sharing the laboratory with all of you during the last two years.

Contents

List of Figures	ix
List of Tables	xi
abbreviation	xii
1 Thesis Introduction	1
1.1 Brain-Computer Interface System	1
1.1.1 Visual Evoked Potentials (VEPs)	2
1.1.2 Motion Visual Evoked Potential	3
1.2 Feature Extraction Methods for VEP	4
1.3 Contributions	4
1.4 Thesis Organization	6
2 Literature Review and Background	8
2.1 Brain-Computer Interface Paradigms: Literature Review	9
2.1.1 Visual Evoked Potential	9
2.1.2 Steady-State Motion Visual Evoked Potential (SSmVEP)	9
2.1.3 Frequency Modulation and Coding Algorithms for SSVEPs	10
2.1.4 Feature Extraction Methods for SSmVEPs	10
2.2 Experimental Pipeline	11
2.2.1 SSmVEP Paradigm Test	12
2.2.2 EEG Data Collection	14

2.2.3	EEG Signal Preprocessing	15
2.3	Frequency Detection: Formulation	15
2.3.1	Spatial Filtering	15
2.3.2	Canonical Correlation Analysis	16
3	Study on Novel Designs with Reduced Fatigue for Steady-State Motion Visual Evoked Potentials	17
3.1	Introduction	17
3.2	Motion Visual Evoked Potential Paradigms	18
3.2.1	Spatial Filtering	21
3.2.2	Frequency Recognition Algorithm	22
3.2.3	Performance Evaluation	23
3.3	Experimental Results	23
3.3.1	Results and Discussions on Different Paradigms	25
3.4	Summary	27
4	DF-SSmVEP: Dual Frequency Aggregated Steady-State Motion Visual Evoked Potential Design with Bifold Canonical Correlation Analysis	28
4.1	Introduction	29
4.2	The Proposed DF-SSmVEP	31
4.2.1	Proposed BCCA Paradigm	34
4.2.2	Experimental Setup	35
4.3	Result	39
4.4	Summary	40
5	Deep Video Canonical Correlation Analysis for Steady State motion Visual Evoked Potential Feature Extraction	41
5.1	Introduction	41
5.2	Methods and Materials	42
5.2.1	Stimulation Design	42

5.3	Deep Video Canonical Correlation Analysis (DvCCA)	44
5.3.1	Initial Weight Extraction from Videos	44
5.3.2	The DvCCA Network Architecture	45
5.4	Experimental Results	46
5.4.1	Experimental Setup	46
5.4.2	Experimental Protocol	47
5.4.3	Result	47
5.5	Summary	49
6	Summary and Future Research Directions	50
6.1	Summary of Thesis Contributions	50
6.2	Future Research	53
	Bibliography	57

List of Figures

Figure 1.1	Illustrative BCI and AR integrated platform [77,78].	3
Figure 1.2	Representation of ERP components. [79]	5
Figure 2.1	Closed loop system used to assess the SSmVEP paradigms and consecutively update them.	13
Figure 2.2	The figure shows the headset used in data collection step.	14
Figure 3.1	(a) Circle-based SSMVEP paradigm. (b) Luminance contrast ratio of the colors used in the designed Circle-based SSMVEP paradigm.	19
Figure 3.2	(a) Square-based SSMVEP paradigm. (b) Luminance contrast ratio of the colors used in the designed Square-based SSMVEP paradigm.	20
Figure 3.3	(a) The PSD plot based on Circle-based SSMVEP with 6.75 Hz target fre- quency. (b) Similar to (a) but with 8.75 Hz target frequency. (c) The PSD plot based on Square-based SSMVEP with 6.75 Hz target frequency. (d) Similar to (c) but with 7.75 Hz target frequency.	24
Figure 3.4	Accuracy comparison results based.	25
Figure 3.5	ITR comparison results.	25
Figure 3.6	Accuracy reduction between first and last sessions.	27
Figure 4.1	Proposed DF-SSmVEP paradigm developed by concurrent inclusion of two types of the motion (rotation and resizing).	30
Figure 4.2	(i) Comparison between existing SSVEP frequency modulation schemes ((a) and (b)) with SSmVEP (c), and the proposed DF-SSmVEP (d). (ii) Luminance contrast ratio of the colors used in the designed DF-SSmVEP.	32

Figure 4.3	Mean and standard deviation across all subjects for each time window: (a) Accuracy comparisons. (b) ITR comparisons.	36
Figure 4.4	(a) The PSD plot based on aggregated SSmVEP with 6-9.5Hz target frequencies. (b) Similar to (a) but with 8-6.5Hz target frequencies.	37
Figure 5.1	The four designed SSmVEP paradigms: (a) Reciprocal-Rotation; (b) Radial-Zoom; (c) Swing; (d) Sway.	43
Figure 5.2	Architecture of the proposed Deep Video Canonical Correlation Analysis (DvCCA).	44
Figure 5.3	Comparison of accuracy and Information Transfer Rate (ITR) across four different SSmVEP paradigms: (a) Mean and standard deviation of SSmVEP recognition accuracy comparisons. (b) ITR of different target identification methods across the 10 subjects.	48
Figure 6.1	A sample of the designed MVEP paradigm.	54
Figure 6.2	A sample of the designed paradigm where logos of specific companies are inserted oscillating with the same frequency.	55

List of Tables

Table 4.1	Mean accuracy (%) and mean ITR (bits/min) comparison between four methods of spatial filtering across the three motions. The best ITR among different time-windows are reported for each filter. Maximum Contrast Fusion (MCF) [44] and T-F Image Fusion [42] are two types of spatial filtering.	37
Table 4.2	Comparison between mean and standard deviation values associated with performance indices (precision, sensitivity, specificity, and accuracy across) all runs for 3 paradigms, i.e., Rotation (R), Radial Zoom (RZ), and the proposed DF-SSmVEP (denoted by DF).	38

Abbreviation

<u>Abbreviation</u>	<u>Description</u>
BCI	Brain Computer Interface
VEP	Visual Evoked Potential
EEG	electroencephalogram
SSVEP	Steady-State Visual Evoked Potential
AR	Augmented Reality
SSmVEP	steady-State motion Visual Evoked Potential
SP	Signal Processing
AI	Artificial Intelligence
ITR	Information Transfer Rate
mVEP	motion Visual Evoked Potential
CCA	Canonical correlation Analysis
MCF	Maximum Contrast Fusion
PSD	Power Spectral Density
DF-SSmVEP	Dual Frequency Aggregated steady-state motion Visual Evoked Potential
BCCA	Bifold Canonical Correlation Analysis
FSK	Frequency-Shift Keying
LCR	Luminance Contrast Ratio
R	Rotation
RZ	Radial Zoom
Fpz	Frontal Position

ANOVA	One-way Analysis of Variance
PI	Performance Indices
DVCCA	Deep Video Canonical Correlation Analysis
VFE	Video Feature Extractor
TRCA	Task Related Component Analysis
RNN	Recurrent Neural Networks
CNN	Convolutional Neural Networks
FFT	Fast Fourier Transform
ReLU	Rectified Linear Unit
ERP	Event-Related Brain Potential
SNR	Signal to Noise Ratio
GAN	Generative Adversarial Network
RL	Reinforcement Learning
ML	Machine Learning
SOA	Stimulus onset asynchrony
TOJ	Temporal-order judgment

Chapter 1

Thesis Introduction

1.1 Brain-Computer Interface System

Throughout history, scientists and engineers have envisioned that interactions between our brain and the outer world can be established without the intervention of human's voluntary nervous system. Dedicated determination towards achieving this goal has resulted in the emergence of Brain-computer-interface (BCI) systems controlling external devices directly using brain signals independently of peripheral nerve pathways [31, 49, 50]. BCI systems have rapidly found their path in clinical studies sparked the development of rehabilitation and assistive BCI technologies [51, 52] as well as diagnosis/prognosis of neurological disorders [32, 33]. Providing comfortable, convenient, cost-effective, and user-friendly BCI platforms are critically challenging for rehabilitation systems [53]. To this end, nowadays, one of the main tendencies of neurotechnology companies is to incorporate Augmented Reality (AR) within BCI technologies [10], which further necessitates the development of advanced signal processing/learning models for BCI systems. The thesis's focus is on incorporation of BCI within an Augmented Reality (AR) [16, 17] platform to provide a means for individuals with communication disabilities to interact with the outer world, e.g., to select an object of interest within the AR environment. The communication can be personalized according to the user's current context and the AR system can be adopted based on changing environments.

Brain-Computer Interface Structure: Generally speaking, BCI systems are communication platforms used to directly translate brain signals to the computer's language so that the system can execute some control commands in the outer world. To put it another way, the system translates brain signals (inputs) to the actions (outputs) without using the whole nervous system. Fig. 1.1 shows an illustrative BCI and AR integrated platform, which consists of four main components. The first part includes showing stimuli on display. These stimuli can be different types of paradigms designed for specific applications. The second part corresponds to the signal acquisition block collecting the brain signals, i.e., EEG signals. The third component is the signal processing module aiming to translate the noisy signals collected in a real-time fashion. Lastly, the computer performs control-commands derived from translated brain signals, which are understandable to the computer. These commands are utilized to control an external devices. The described BCI systems has a wide range of applications such as:

- **Neuroprosthesis** is a device to overcome neuro-disabilities caused by injuries. In other words, these devices are meant to replace cognitive motor or sensory abilities of an organism.
- **P300 Speller** is a system developed so that users can input texts to a computer through brain signals and without using their limbs.
- **Neurogaming** is a type of gaming that deploys BCI systems in such a way that users interact with the gaming platform without the intervention of traditional sensory controllers.
- **Neuro-marketing and Advertising** is a new field of marketing deploying different neuroimaging modalities to better understand the customer's reaction to marketing stimuli.

1.1.1 Visual Evoked Potentials (VEPs)

The key reason for the recent surge of interest in VEPs [57] is their easy system configuration, which currently provides the fastest and the most reliable communication paradigm for implementing a non-invasive BCI. In this context, BCI technologies developed via EEG-based steady-state visually evoked potential (SSVEP) [19, 20] have been the main research target in recent years due to their high achievable Information Transfer Rate (ITR), the minimal requirement for user training,

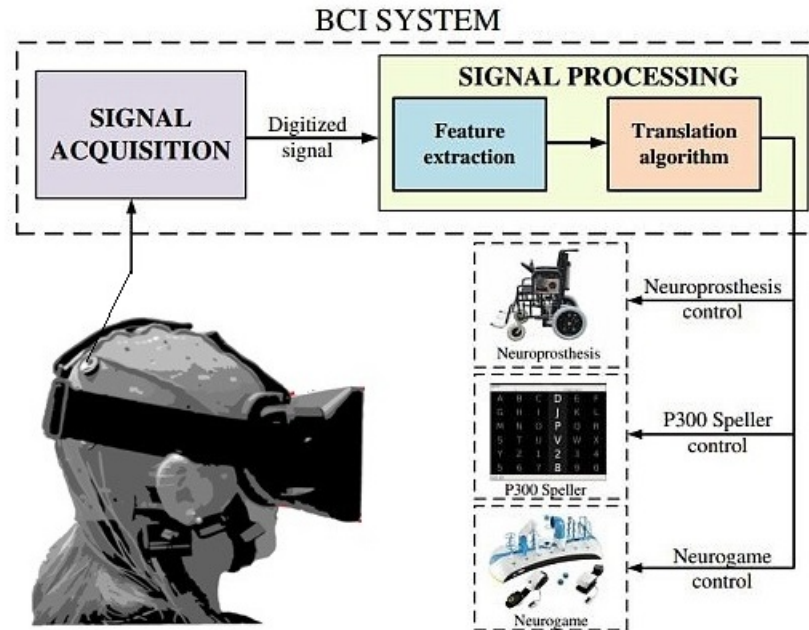


Figure 1.1: Illustrative BCI and AR integrated platform [77, 78].

and excellent interactive potential, such as high tolerance to artifacts and robust performance across users. In a typical SSVEP-based BCI system, the virtual object flickers with a specific frequency while the processing module extracts the effect of the flickering frequency on the EEG signals.

Continuous utilization of SSVEPs causes eye fatigue and puts an excessive mental load on subjects [56] rendering its practical utilization challenging. To address this issue, Motion-Onset Visual Evoked Potentials (mVEPs) [41, 57, 58], which elicit $P1$, $N2$, and $P2$ components in the EEG signals are introduced as attractive alternatives.

1.1.2 Motion Visual Evoked Potential

Recently, there has been a surge of interest on Steady-State motion Visual Evoked Potentials (SSmVEPs) [59] benefiting from advantages of both mVEPs and SSVEPs. The SSmVEPs comprise of reversal periodic movements such as Contraction-Expansion, Rotation, Swing, and Radial-Zoom [28, 44], which are used instead of conventional flickering-based stimuli.

1.2 Feature Extraction Methods for VEP

One of the main challenges of the use of raw EEG recording is to detect a reliable pattern of neural activity with a source of cognitive mechanisms [79]. In other words, robust features related to cognitive tasks need to be extracted from EEG signals. In that way, various features have been recognized in the cocktail-party type and noisy EEG signals when it comes to VEPs. Event-Related Potential (ERP) represented in Fig. 1.2 is a group of time-related components evoked in the EEG signal in response to visual stimulations. Viewing any sudden movements, pictures, or words displayed on the screen elicits ERPs after relatively fixed delays in time. Hence, instead of tracking the whole signal to find the features, we can focus on specific time stamps after displaying visual stimuli. ERPs appear in the visual cortex, especially in the occipital lobe. Basically, ERPs consist of four main components:

- **P1 or P100**, which is the first positive peak linked with low-level perception. It automatically appears around 100 ms after the onset of any target.
- **N1 or N100** is a negative peak linked with low-level perception. It automatically peaks between 80 and 120 after the onset of any target.
- **P2 or P200** is a post-synaptic waveform component distributed around the centro-frontal and the parieto-occipital areas of the scalp. It positively peaks around 200 ms after the onset of stimuli.
- **N400** is a brain response to conscious cognitive processing such as semantically anomalous materials. As a result, a large negative peak is elicited in the signal around 400 ms after the display of targets.

1.3 Contributions

The main goal of the thesis research work is to address the following key question: “*What does the incorporation of Visually Evoked Potentials (VEP) extracted from Electrophysiological (EEG) signals mean for BCI-based Assistive Technologies?*”. The abundance of the EEG signals collected

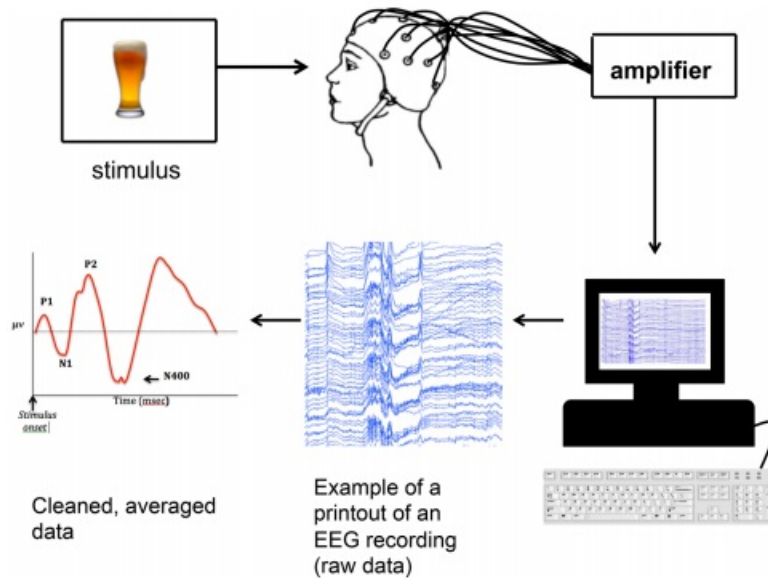


Figure 1.2: Representation of ERP components. [79]

through a BCI system compels complex signal and information processing to isolate desired features from EEG signals that represent the user's intention to communicate or drive a particular command.

Nowadays, conventional SSmVEP paradigms, including Newton Rings and motions with high-contrast colors, are used in BCIs designed for assistive technology. Permanent use of these devices may cause some side-effects for the patients. One of this project's main motivations was to help the industry to replace typical motions with graphical motions, which are more user-friendly in terms of colors and complexity. This way, we can enhance both the performance as well as the practicality of these technologies.

The most important contributions of the thesis are summarized as follows:

- (1) **Study on Novel Designs with Reduced Fatigue for Steady-State Motion Visual Evoked Potentials [61]:** Two Novel flicker-free SSmVEP paradigms derived from an ongoing experiment are proposed. The proposed paradigms are selected from the many paradigms tested on real subjects and chosen for application of real BCI within AR context. Moreover, the visual fatigue level is optimized during the test for the selected designs. One of the proposed paradigms even outperformed a typical SSVEP, which is a benchmark in terms of accuracy. To the best of our knowledge, this is the first time that robust SSmVEP paradigms with the

least visual fatigue can get better performance than SSVEPs.

- (2) **DF-SSmVEP: Dual Frequency Aggregated Steady-State Motion Visual Evoked Potential Design with Bifold Canonical Correlation Analysis [63]:** A new form of SSmVEPs is proposed based on integrating individual SSmVEPs. To this end, we generate a novel idea of design by modulating two frequencies within a single target. A combination of different motion modes, more than one modulated frequencies within a single paradigm can lead to a robust and quick system. The constituent SSmVEP paradigms were not individually applicable to the BCI system; however, the integrated paradigm, referred to as the DF-SSmVEP, becomes robust enough to be utilized in BCI systems. Secondly, a new spatial filtering approach, BCCA, is proposed for classifying DFSSmVEPs. The new BCCA outperforms regular CCA because it is highly compatible with the design of emerging DFSSmVEP.
- (3) **Deep Video Canonical Correlation Analysis for Steady-State motion Visual Evoked Potential Feature Extraction [62]:** These days, most of the existing algorithms are black boxes without any intuition in the emerging field of deep learning. According to the literature, one of the best frequency classifier used within the SSmVEP-based BCIs are CNNs. A new deep learning-based algorithm is proposed that outperforms the CNN-based benchmark for classification. The proposed model's architecture provides a higher interpretation providing insights on the reasons behind achieved superior results. As another contribution, it is the first time that a model can directly discover the connection between videos and EEG signals in visual BCIs. This can be the first step to reversely solve the problem and understand the connection between VEP's intensity and the stimuli' shape.

1.4 Thesis Organization

The rest of the thesis is organized as follows:

- Chapter 2 provides an overview of the literature on various VEP paradigms as well as different classifiers used in this context. Additionally, in this chapter, we present the background and relevant EEG signal processing pipelines required to follow the thesis's advancements.

- Chapter 3 proposes novel flicker-free SSmVEP paradigms that address the key issue of conventional light-flashing SSVEP. In this chapter, the proposed paradigms incorporated within an experimental BCI system are compared to SSVEPs in terms of visual fatigue, accuracy, and ITR.
- Chapter 4 consists of two parts aiming to enhance the accuracy and speed of SSmVEP paradigms. First, different motion modes within SSmVEPs are designed and concurrently integrated into a single target to create a new type of visual stimulus called Dual Frequency Aggregated steady-state motion Visual Evoked Potential (DF-SSmVEP). Secondly, an innovative way of target frequency modulation is introduced in DF-SSmVEPs.
- Chapter 5 targets EEG signal processing step of SSmVEP-based BCI system. To that end, a supervised frequency detection module deploying videos of stimulation directly is introduced. The proposed Neural Network-based model considerably competes against recently proposed state-of-the-art Convolutional Neural Network-based models.
- Chapter 6 wraps up the thesis and illustrates some directions for future works.

Chapter 2

Literature Review and Background

Despite recent advances in Signal Processing (SP), Artificial Intelligence (AI), and computational technologies, our brain is considered as the most intriguing signal processing unit in existence. Plasticity property of the brain, i.e., the ability of neurons to modify their behavior (form and function) in response to environmental changes, has very recently [1, 2] allowed researchers to give three paralyzed patients the astonishing chance of walking again (even taking a few steps). Essentially, the plasticity property of our brain has motivated development of Brain-Computer Interface (BCI) systems [7–11] to provide an alternative form of a communication channel between human brain signals and the outer world. The ultimate goal of a BCI system is to establish a robust communication channel with high throughput and accuracy between the brain and the outer world. The BCI systems have several therapeutic applications of significant importance including but not limited to rehabilitation/assistive systems [6, 7], rehabilitation robotic [12, 13], and neuro-prosthesis control [14]. Despite recent advancements in BCIs, such systems are still far from being incorporated reliably within Human-Machine Inference Networks [15].

Various techniques, ranging from tuning stimulations to developing complicated spatial filtering methods, have been proposed recently to enhance the performance of BCI systems. In this chapter, we will elaborate on the existing approaches utilized to improve VEP-based BCI systems. A qualitative comparison between different techniques is provided in this chapter as well. Moreover, details on the experimental pipeline followed during our tests are provided. Finally, an important formulation and crucial processing modules are illustrated in this chapter.

2.1 Brain-Computer Interface Paradigms: Literature Review

2.1.1 Visual Evoked Potential

Recent technology trends show that leading technology companies are racing to develop advanced BCI systems coupled with Augmented Reality (AR) visors. It is widely expected that AR coupled with BCI would be the next era of computing. Electroencephalogram (EEG)-based BCI systems developed based on Steady-State Visual Evoked Potential (SSVEP) are considered as the main technology for potential integration with AR due to their outstanding characteristics such as high accuracy and Information Transfer Rate (ITR) [17, 54, 55]. Despite the popularity of SSVEPs, their utilization for practical application especially for assistive technologies is complicated and challenging, which can be attributed to the following key issues:

- (i) Eye fatigue when low-frequency flickering lights are used;
- (ii) Higher risk of induced epileptic seizure when medium-frequency flickering lights are used, and;
- (iii) Low signal amplitude when high-frequency flickering lights are used.

2.1.2 Steady-State Motion Visual Evoked Potential (SSmVEP)

To address key the above-mentioned issues associated with SSVEPs, there has been a surge of interest on Steady-State motion-Visual Evoked Potentials (SSmVEP), where motion stimulation is utilized instead of conventional light-flashing/flickering technique. While SSmVEPs are posed to pave the way for the advancement of AR-based BCI systems, there are still in their infancy. Although the BCI systems developed based on SSmVEPs induce less eye fatigue, their frequency detection accuracy, and ITR are not comparable to that of the SSVEPs, yet. In other words, Power Spectral Density (PSD) of the EEG signals when SSVEPs are used spike more intense modulated frequencies in comparison to the case where SSmVEPs are used under similar conditions [61]. In [60], features of the brain response to different flickering images are recognized by modeling visual pathways based on artificial neural networks. SSmVEPs, however, can evoke other harmonic frequencies/features of EEG signals depending on the type of designed motion paradigm due to

their complex nature. The luminance of utilized colors [27], brightness contrast ratio [64], and the existence of sharp edges in the design of SSmVEPs [28,61] are examples of the complexities that can be taken into account for the design of SSmVEPs. These effects can lead to phase shift of evoked potentials, appearance of frequency peaks in the PSD, and other extra informative event-related potential components.

2.1.3 Frequency Modulation and Coding Algorithms for SSVEPs

One issue that is shared by both SSVEP and SSmVEP categories is the challenge of coding more targets under available resources. Within the context of SSVEPs, the following research works have been conducted to address this issue: Reference [38] introduced simultaneous phase and frequency modulations. Reference [39] used modulation in time, i.e., lengthening of the trial duration. Two different flickering-frequencies are shown consecutively for each target. Following a similar path, References [35,36] focused on using more than one frequency in a single target (but not at the same time) via Frequency-Shift Keying (FSK) modulation, also referred to as code modulation, i.e., trial time is again used for modulation purposes. Similarly, Reference [37] used code modulation with a single frequency for each target but with different phase shifts over one trial to enhance the system. Such code-VEPs [35–37,40] and phase modulation [37,38] techniques are, however, very sensitive to synchronization, and as trial time is used for modulation purposes, ITR will be compromised. When it comes to SSmVEPs, the issue of coding more targets with enhanced ITR has not yet been considered, the thesis addresses this gap.

2.1.4 Feature Extraction Methods for SSmVEPs

Target identification is a crucial component of a SSmVEP-based BCI system where, conventionally, Canonical Correlation Analysis (CCA) is utilized [65]. The CCA tries to correlate a linear relationship between two multi-dimension variables, i.e., recorded EEG signals and template signals, which are functions of the SSmVEP frequencies. As regular CCA's performance can highly be affected by the interference of spontaneous EEG signals, its extensions, for instance, via spatial filtering are widely considered [34,66]. The Task Related Component Analysis (TRCA) enhancing reproducibility of SSVEPs across multiple trials is another attempt to remove the unrelated

background EEG activities [67]. In certain cases, CCA becomes weak in exploiting useful representatives of the underlying EEG data due to its nonlinearity. Kernel-based CCA is a solution to nonlinearly project data to an embedding space, in which the linear CCA can be applied [68]. Furthermore, nonlinearity map of data can be generated from the template signals in a supervised fashion, and it was the first intuition to use the Recurrent Neural Networks (RNN) before applying CCA in SSmVEPs [71] or SSVEPs [69, 70]. Recent studies have shown that Convolutional Neural Networks (CNNs) can boost performance of BCI classifiers [72, 73]. In Reference [74], for instance, a new CNN method is applied to the complex Fast Fourier Transform (FFT) of EEG signals exploiting magnitude and phase information and outperforming CCA-based solutions. Using deep networks to find similarities between test and template signals, however, can lead to the overfitting issue due to small size of training datasets, typically, available for SSmVEPs-based training.

2.2 Experimental Pipeline

In this section, the principal steps used in our data collection sessions are explained. Moreover, we elaborate on the cycle of testing and updating BCI paradigms designed by our team of designers from the art department. To investigate the impact of deploying a new theory or a particular paradigm design on BCI systems' performance, it is important to simulate the BCI system applied to real subjects. To that end, we collect largely real EEG signals under special circumstances. Because of the existence of artifacts including biological signal interference, eye blinks, eye movement, cardiac activity, muscle activity, and environmental noise, EEG signals are subject to significant distortions. Additionally, some of the BCI tests are relatively complex, so the participants need to be trained beforehand. Low level of concentration and environmental distractions modeled in the background noise are other factors that inevitably occur in data collection.

The comparison between different SSmVEP paradigms or different frequency identification algorithms should not be biased towards the aforementioned artifacts. To draw a fair comparison, the number of collected EEG signals should be large enough. In other words, several subjects usually participate in each experiment and the tests are repeated several times for each individual to make sure that the results are significant. However, for analysis of prototype paradigms, we test our VEP

paradigms on a small group of subjects (one or two). Then, those paradigms, which get the highest scores during initial tests will be used in the large-scale experiment.

The datasets used in different experiments of the thesis are collected using different setups. Hence, in what follows, we provide general protocols pursued during our data acquisition tests. The detailed setup of each test is explained in its corresponding chapter.

It is worth mentioning that each experiment consists of a set of trials in which a target is pointed out. There is a break or resting time between every pair of consecutive trials. . Stimulus onset asynchrony (SOA) is a measure denoting the amount of time between the onset of two consecutive stimuli. A short SOA result in interference in the neural processing of different stimuli. Conversely, a very large SOA may make a trial independent from the next trial and decrease the ITR of the BCI system. To compromise between the ITR of the BCI system and neural processing interference, 3-5 seconds break between trials are set in different experiments. Temporal-order judgment (TOJ) tasks from literature are utilized to investigate the estimated processing time within the brain after displaying visual stimuli. In our experiments, early components of the visual cortex are mainly taken into account without using high-level perceptual organization related to creativity. Therefore, the aforementioned resting range is big enough to avoid interference in the brain's reactions to different stimuli.

2.2.1 SSmVEP Paradigm Test

The novel SSmVEP paradigms designed through this thesis research are the output of a closed-loop system. In this system, the inputs are stimulation videos, and the output is a final score given to the stimulation. Additionally, designers using these scores decide to alter the characteristics of the paradigms based on known tips from literature. These tips include the effect of different types of SSmVEPs on the evoked harmonics of the EEG signal. As another tip, decreasing the luminance contrast of shapes results in a low fatigue score; however, it comes with the price of having less accuracy and less Information Transfer Rate (ITR).

Fig. 2.1 demonstrates the block diagram of our experimental pipeline to create exceptional SSmVEP paradigms leading to high performance, as well as least visual fatigue. The diagram consists

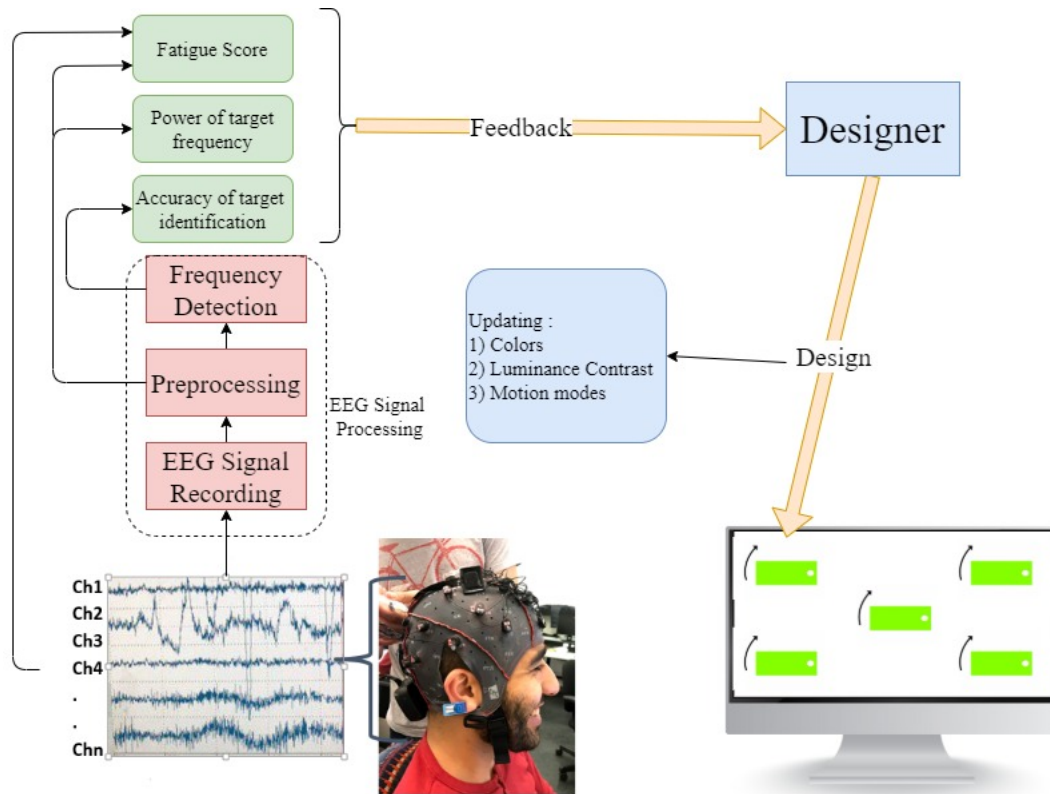


Figure 2.1: Closed loop system used to assess the SSmVEP paradigms and consecutively update them.

of two main blocks, including EEG Signal Processing and Designing block. The first block, including EEG signal acquisition, preprocessing, and frequency detection, is fed with recorded EEG signals, which provides a score in return. The score is based on three main criteria: fatigue score, power of signal within target frequencies, and accuracy of the frequency detection module. Moreover, the fatigue score covers both a score asked of each subject directly as well as the drop in accuracy during the consecutive trials. A designer block is a group of designers who change the paradigms based on the previous block's feedback so that the next total score increases. In other words, the term "designer" denotes a team of researchers who manually manipulate the characteristics of paradigms. The update applied to the paradigms is taken place experimentally. There are three ways to alter the paradigms: (i) Changing the colors used in the paradigm or background; (ii) Tweaking the brightness of the videos and Luminance Contrast of the colors; (iii) Replacing the



Figure 2.2: The figure shows the headset used in data collection step.

motion modes (i.e., contraction-expansion, and rotation). Next, we will elaborate on the modules of the EEG signal processing block.

2.2.2 EEG Data Collection

A portable and wireless biosignal acquisition system, g.Nautilus from g.tech Medical Engineering [48], was used to collect EEG signals. The g.tech system shown in Fig. 2.2 consists of a cap with 32 bipolar active wet electrodes with 24 Bit resolution, and a sampling rate of 500Hz. The ground electrode was placed at the earlobe during all experiments. In the g.Nautilus headset, there is a bio-potential amplifier with prefixed electrode stands labeled with a number and a letter. In these labels, letters represent the initials of the brain's lobe where the corresponding electrode are placed. The number in the electrodes' labels correspond to the positions defined by the international 10-20 system [80].

2.2.3 EEG Signal Preprocessing

EEG signals are the common neuroimaging modalities used in BCI systems. However, EEG waveforms are usually contaminated by artifacts, and drift-noise, so it is hard to distinguish between the noise and the provoked potentials caused by the BCI system. Hence, the preprocessing step should affect raw EEG signals fed to machine learning algorithms to ease the signal classification task [81]. First of all, power line noise (60 Hz) is removed with a notch filter during the data collection, followed by the Chebyshev-II filter of order 10 to select a frequency-band within 0.5 to 100 Hz.

Generally speaking, the eyes and visual system are behave like a low-pass filter, so we cannot realize high-frequency alteration happening in the environment. The frequency-band signatures of visual responses targeted in this thesis are confided to 60 Hz. Hence, another band-pass filter (usually within 0.5 to 50 Hz) is applied to the signals during the offline preprocessing. It is worth mentioning that a lower bound for the filter is set so that the drift-noise is filtered. After time-domain filtering of the signal, we send it to the “Spatial Filtering” module, which is described next.

2.3 Frequency Detection: Formulation

2.3.1 Spatial Filtering

EEG signals, recorded from the surface of the scalp, are exposed to signal interference. Thus, the output is the superposition of multiple signals from different sources including the SSVEP signals. The SSVEP signal is concentrated generally in the occipital lobe (especially Oz electrode). However, there are informative data in other electrodes, which can be used to remove unrelated waveforms in the frequency-band of targets. A reasonable approach to use the information of other electrodes is to form a weighted average on the recording channels and construct a single composite signal. The method of linearly integrating multi-channel into single-channel is referred to spatial filtering in the context of SSVEPs.

2.3.2 Canonical Correlation Analysis

Canonical Correlation Analysis (CCA) is a statistical method utilized to study the linear relationship between two groups of multi-dimensional variables. For two sets of signals arranged in matrices denoted by \mathbf{X} and \mathbf{Y} , the goal is to find two linear projection vectors \mathbf{w}_x and \mathbf{w}_y , such that the linear combination of the two groups of signals $\mathbf{w}_x^T \mathbf{X}$ and $\mathbf{w}_y^T \mathbf{Y}$ has the largest correlation coefficient, i.e.,

$$\rho = \max \frac{E(\mathbf{w}_x^T \mathbf{X} \mathbf{Y}^T \mathbf{w}_y)}{\sqrt{E(\mathbf{w}_x^T \mathbf{X} \mathbf{Y}^T \mathbf{w}_x) E(\mathbf{w}_y^T \mathbf{X} \mathbf{Y}^T \mathbf{w}_y)}}. \quad (2.1)$$

Conventionally, the reference signals are constructed at the stimulation frequency f_i as (*in contrary, the proposed DvCCA uses a deep architecture to construct reference signals*)

$$\mathbf{y}_i = [\cos 2\pi f_i t, \sin 2\pi f_i t, \dots, \cos 2\pi N_h f_i t, \sin 2\pi N_h f_i t]^T,$$

where $t = \frac{1}{f_s}, \dots, \frac{m}{f_s}$, the f_s is the sampling rate, m is sample points, and N_h is the number of harmonics, which is dependent on the paradigm, and is obtained experimentally from the Welch Power Spectrum of signals.

Chapter 3

Study on Novel Designs with Reduced Fatigue for Steady-State Motion Visual Evoked Potentials

3.1 Introduction

The chapter focuses on incorporation of Brain-Computer Interfacing (BCI) within an Augmented Reality (AR) platform to provide means for individuals with communication disabilities to interact with the outer world. As stated previously, there has been a recent surge of interest on Steady-State Visual Evoked Potentials (SSVEP). In a typical SSVEP-based BCI system, the virtual object within the AR environment flickers with a specific frequency while the signal processing module extracts the effects of the flickering frequency on the Electrophysiological (EEG) signals. Despite the popularity of SSVEPs, their utilization for practical application especially for assistive technologies is complicated and challenging due to eye fatigue and risk of induced epileptic seizure. In this regard, the key issue being targeted in this chapter is addressing fatigue of the flicker (or brightness modulation) by development of flicker-free Steady-State motion Visual Evoked Potential (SSMVEP). Two novel SSMVEP paradigms, i.e., Square-based and Circle-based paradigms, with

low luminance contrast and oscillating expansion and contraction motions are designed, and integrated within a BCI system. Through experimental evaluations, high detection accuracy of 95.31% is achieved for the square-based SSMVEP.

The rest of the chapter is organized as follows: Section 3.2 introduces the proposed SSMVEP paradigms. Section 3.3 presents the experimental results. Finally, Section 3.4 concludes the chapter.

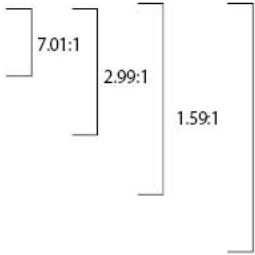
3.2 Motion Visual Evoked Potential Paradigms

To address the issues with SSVEP, mentioned in Sub-section 2.1.1, and in particular unacceptability of flicker (or brightness modulation), the chapter focuses on development of motion Visual Evoked Potential (mVEP) [21, 44]. What is unknown is the various responses of the brain, to differing visual images, geometric patterns, colour variation, and image motion under normal environmental conditions. In this regard, the chapter develops/implements two novel and innovative motion stimuli together with processing and learning algorithms for inducing discriminative mVEPs and associating the EEG signals to target class. More specifically, to understand the nature of mVEPs, two innovative motion stimuli with oscillating expansion and contraction motions, as alternative solutions to the recently proposed mVEP, are designed, investigated, and their effectiveness to provide a high-refresh-rate display for visual stimuli is evaluated. To further understand the behavior of designed motion patterns, initial set of real-data collection and analysis are performed and EEG responses are captured/analyzed under different frame rates and various scenarios using a 32 channel EEG headset. Based on real-world collected set of test data, pre-processing and feature extraction on the collected EEG signals in response to the motion stimuli are performed to uniquely identify the intention of the subject.

More specifically, two contraction-expansion paradigms as shown in Figs. 3.1 and 3.2 are designed, referred to as Circle-based SSMVEP paradigm (Fig. 3.1), and Square-based SSMVEP paradigm (Fig. 3.2). The motion stimuli design is based on contraction-expansion with two shapes (a circle and a square) modulated at four frequencies (6.75, 7.75, 8.75, and 9.75 Hz). Each paradigm consists of two parts. The first part is a contraction-expansion ring, and the second part is a shape located in the center of the stimulus resizing with a constant frequency. In the contraction-expansion



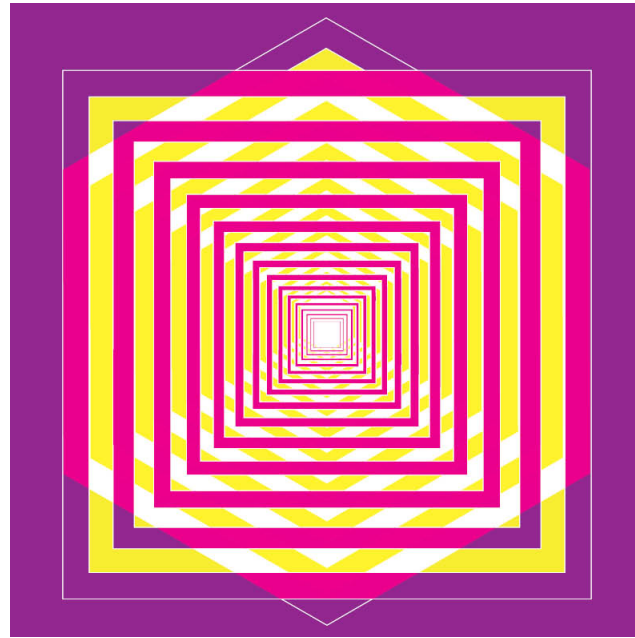
(a)

Color	Luminance	Contrast Ratio
 #00a79d	56%	
 #000000	0%	
 #ffffff	100%	
 #c9415e	50%	
 #3a373a	22%	

(b)

Figure 3.1: (a) Circle-based SSMVEP paradigm. (b) Luminance contrast ratio of the colors used in the designed Circle-based SSMVEP paradigm.

segment, the frequency of motion direction change is defined as motion inversion frequency [27]. Moreover, the second segment of the paradigm resizes with motion inversion frequency. Motion inversion frequency is adopted as the fundamental frequency of the SSmVEP in the EEG signal. However, the frequency of shape-size modulation is equal to the half-frequency of the SSMVEP [28]. In other words, we created the paradigms in which one piece evokes first frequency harmonic of SSmVEP, and another piece evokes half frequency harmonic of the SSmVEP. The key focus of



(a)

Color	Luminance	Contrast Ratio
 #91278f	42%	$\left. \begin{array}{l} \left[\begin{array}{l} 5.94:1 \\ 1.68:1 \end{array} \right] \right\} 7.26:1$
 #f9ed33	89%	
 #ea008c	56%	
 #ffffff	100%	

(b)

Figure 3.2: (a) Square-based SSmVEP paradigm. (b) Luminance contrast ratio of the colors used in the designed Square-based SSMVEP paradigm.

these designs is that the luminance contrast of the colors used in these paradigms (between background and image, rings, and shapes) is relatively low (maximum color contrasts are 7.26:1 and 7:01:1 where the contrast levels of the black and white patterns with high brightness are approximately 13.9:1). The Luminance contrast are defined according to ISO-9241-3 and ANSI-HFES-100-1988 [29].

The two square-based and circle-based paradigms are used as SSmVEPs for EEG data collection and analysis. To remove the unwanted signal components, first zero-phase Chebyshev Type I

band-pass filter (2-40 Hz) is applied to EEG signals to smooth the data and remove high-frequency artifacts. The next step is spatial filtering, which is described in the next sub-section.

3.2.1 Spatial Filtering

In this thesis, Maximum Contrast Fusion (MCF) technique is used for spatial filtering. More specifically, for a visual stimulus with frequency f_o , the SSmVEP signal recorded by the i^{th} electrode can be expressed as

$$y_i(t) = \sum_{j=1}^{N_h} a_{i,j} \sin(2j\pi f_o t + \phi_{i,j}) + v_i(t), \quad (3.1)$$

where N_H is the number of harmonics, and terms $a_{i,j}$ and ϕ_i represent the amplitude and phase of the j^{th} harmonic component, respectively. The model in Eq. (3.1) decomposes the signal into sum of the SSmVEP induced by the visual stimulus and additive noise $v_i(t)$ to represent uncertainties of the model. Eq. (3.1) can be expressed in vectorized format as follows

$$\mathbf{y}_i = \mathbf{s}_i + \mathbf{v}_i \quad (3.2)$$

$$\text{where } \mathbf{s}_i = [\mathbf{a}_i^T \mathbf{X}]^T, \text{ with } \mathbf{X} = [\mathbf{x}_1, \dots, \mathbf{x}_{N_h}], \quad (3.3)$$

where superscript T represents transpose operator; Vector \mathbf{x}_i , for $(1 \leq i \leq N)$, consists of $\sin(2n\pi f_o t)$ and $\cos(2n\pi f_o t)$ components; N represents the number of harmonics, and; vector \mathbf{a}_i represents the amplitude of SSMVEP at its stimulus frequency and harmonics. The recorded signals from N_{ch} channels are combined in matrix $\mathbf{Y} = [\mathbf{y}_1, \dots, \mathbf{y}_{N_{ch}}]$, where each column corresponds to signals collected from one of the N_{ch} electrodes channel. The observation matrix \mathbf{Y} can be projected to the SSMVEP space through a projection matrix [26] defined as $Q = \mathbf{X}(\mathbf{X}^T \mathbf{X})^{-1} \mathbf{X}^T$. Thus, the noise signal can be expressed as $\mathbf{Y}' = \mathbf{Y} - Q\mathbf{Y}$. Assuming that the weighting coefficient for each channel is w , then the SSmVEP signal energy can be approximated as

$$\|\mathbf{Y}\mathbf{w}\|^2 = \mathbf{w}^T \mathbf{Y}^T \mathbf{Y} \mathbf{w}. \quad (3.4)$$

The maximum contrast fusion obtains the spatial filter coefficients w by maximizing the SSmVEP energy and minimizing the noise energy, i.e.,

$$E = \max \frac{\mathbf{w}^T \mathbf{Y}^T \mathbf{Y} \mathbf{w}}{\mathbf{w}^T \mathbf{Y}'^T \mathbf{Y}' \mathbf{w}}, \quad (3.5)$$

which can be solved by the generalized eigenvalue decomposition of $\mathbf{Y}^T \mathbf{Y}$ and $\mathbf{Y}'^T \mathbf{Y}'$. The eigenvector corresponding to the largest eigenvalue is the required spatial filter coefficient.

3.2.2 Frequency Recognition Algorithm

In this work, the Welch Power Spectral Density (PSD) is used to estimate random signals by dividing data with a length of N into M segments of length L . Its window averaged period formula is given by

$$P(w) = \frac{1}{M} \sum_{i=1}^M \left[\frac{1}{LP_0} \left| \sum_{n=1}^L w(n) x_i(n) e^{-jwn} \right|^2 \right], \quad (3.6)$$

where p_0 refers to the power of window $w(n)$ given by

$$P_0 = \frac{1}{L} \sum_{n=1}^L |w(n)|^2. \quad (3.7)$$

Canonical Correlation Analysis

Canonical correlation analysis is a statistical method to study the linear relationship between two groups of multidimensional variables, which extends the simple correlation analysis to two groups of variables. For the two sets of signals \mathbf{X} and \mathbf{Y} , the goal is to find two linear projection vectors \mathbf{w}_x and \mathbf{w}_y , such that the linear combination of two groups of signals $\mathbf{w}_x^T \mathbf{X}$ and $\mathbf{w}_y^T \mathbf{Y}$ has the largest correlation coefficient computed as follows

$$\rho = \max \frac{E(\mathbf{w}_x^T \mathbf{X} \mathbf{Y}^T \mathbf{w}_y)}{\sqrt{E(\mathbf{w}_x^T \mathbf{X} \mathbf{Y}^T \mathbf{w}_x) E(\mathbf{w}_y^T \mathbf{X} \mathbf{Y}^T \mathbf{w}_y)}}. \quad (3.8)$$

The reference signals were constructed at the stimulation frequency f_i as follows

$$\mathbf{y}_i = [\cos 2\pi f_i t, \sin 2\pi f_i t, \dots, \cos 2\pi N_h f_i t, \sin 2\pi N_h f_i t]^T, \quad (3.9)$$

where $t = \frac{1}{f_s}, \dots, \frac{m}{f_s}$, and N_h is the number of harmonics, which is dependent on the utilized paradigms. The f_s is the sampling rate, and m is sample points. Number of harmonics were obtained experimentally from Welch Power Spectrum of signals.

3.2.3 Performance Evaluation

Classification accuracy and ITR evaluate the performance of the paradigms. Information Transfer Rate is a valid criterion to assess the speed of BCI systems. The ITR is computed as follows

$$\text{ITR} = \frac{60}{T} \left[\log_2 K + \sigma \log_2 \sigma + (1 - \sigma) \log_2 \left(\frac{1 - \sigma}{K - 1} \right) \right], \quad (3.10)$$

where T is the sum of time of each trial and the resting state time between two trials, K is the number of stimuli, and σ is the recognition accuracy. Additionally, the accuracy-difference between trials of two consecutive sessions can be used as an effective assessment tool to measure the fatigue associated with a designed paradigm.

3.3 Experimental Results

In this section, first, we present the dataset collected and utilized to assess the efficiency of the two proposed paradigms. The collected dataset consists of 16 trials for each target-frequency per subject. Two novel motion-SSVEP with low luminance contrast between colors and one checkerboard flickering (normal SSVEP) are shown to subjects.

Experimental Environment: In the initial experiments, two individuals, one male and one female (20-27 years old) were recruited with no record/evidence of visual or color-recognition disabilities. The data were collected with the policy certification of Ethical acceptability for research involving human subjects and approved by Concordia University with the certification number 3007997. The procedures used in this protocol are all well established and known to be safe. The EEG signals were collected by electrodes Pz , $Po7$, $Po3$, $Po4$, $Po8$, and Oz from parietal and occipital lobes of the brain. The experiments consisted of four targets displayed simultaneously on a 21.5-inch LED screen with a green background. The resolution of the screen was 1920×1080 at 60Hz refresh rate.

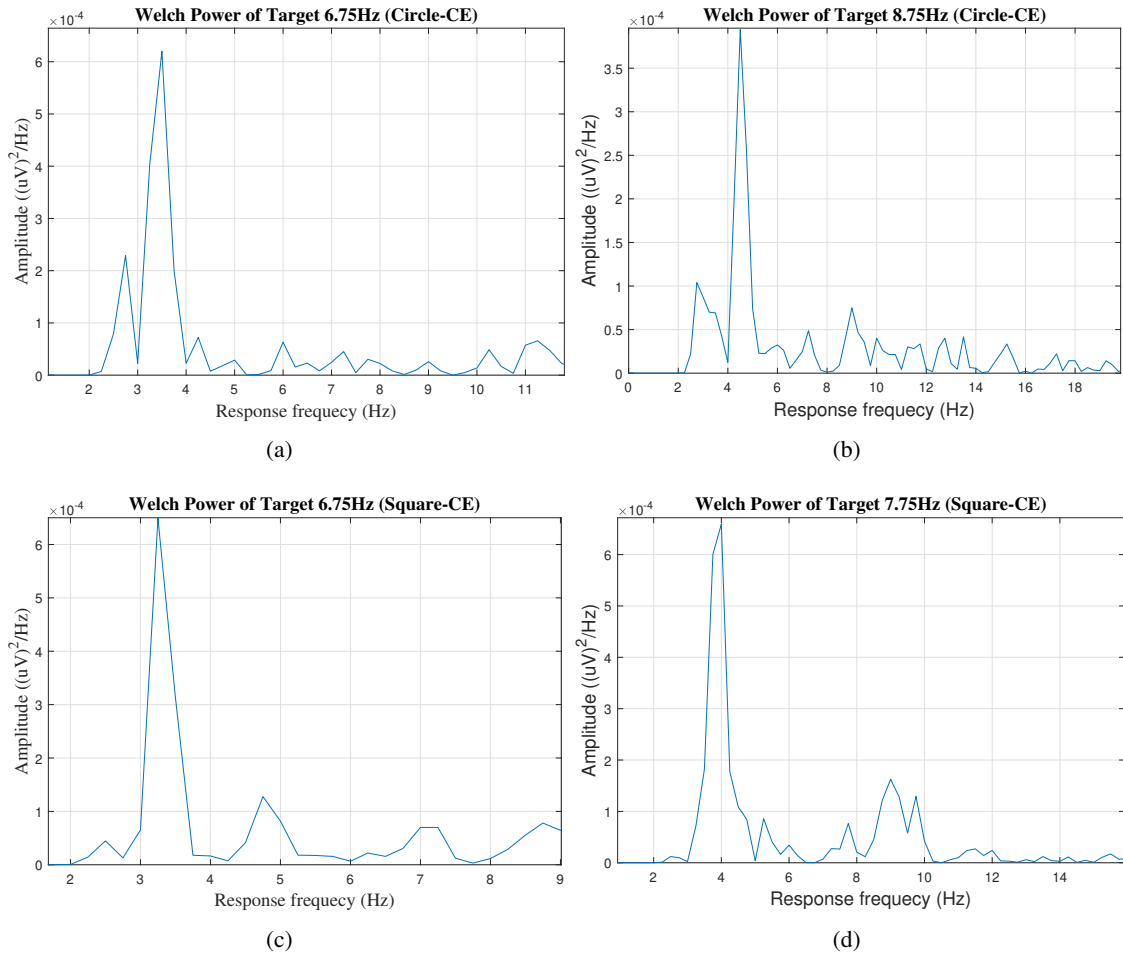


Figure 3.3: (a) The PSD plot based on Circle-based SSMVEP with 6.75 Hz target frequency. (b) Similar to (a) but with 8.75 Hz target frequency. (c) The PSD plot based on Square-based SSMVEP with 6.75 Hz target frequency. (d) Similar to (c) but with 7.75 Hz target frequency.

All the subjects are asked to stare at the stimuli based on the same protocol.

Subjects participated in the test for two rounds with a 10 minutes break between the rounds. Each round included two consecutive sessions. In each session, targets of four frequencies were displayed in four trials. Each trial lasted for 4 seconds with a 3 second break between trials. Fig. 4.4 illustrates the Welch Power Spectral Density (PSD) of the EEG signals collected from different stimulation frequencies for Subject 1. Target frequencies of the stimuli are 6.75, 7.75, 8.75, and 9.75 Hz. It is observed that the proposed paradigms have the ability to evoke expected potentials with the highest PSD amplitudes occurring at the half target frequencies in the SSmVEP paradigms (i.e., 3.4, 3.9, 4.3, and 4.9Hz).

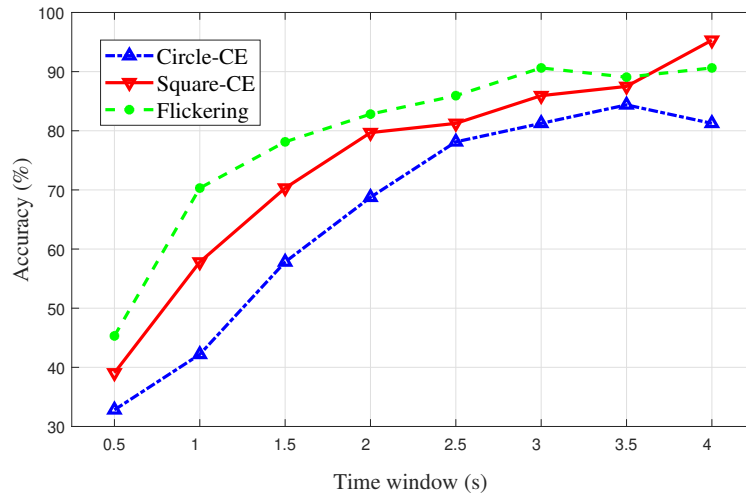


Figure 3.4: Accuracy comparison results based.

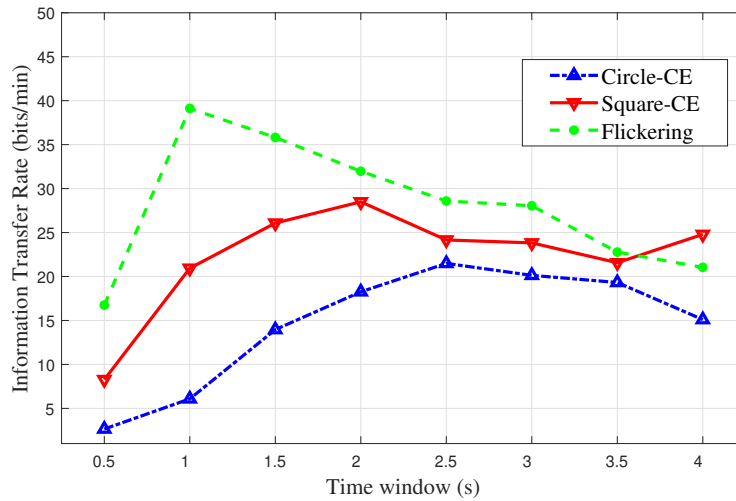


Figure 3.5: ITR comparison results.

3.3.1 Results and Discussions on Different Paradigms

In this sub-section, we present different results and compare the results obtained from the two proposed SSmVEP designs against the conventional flicker-based SSVEP approach. In particular, comparisons are performed over the following three aspects: (i) Classification accuracy; (ii) Information transfer rate of different paradigms, and; (iii) Accuracy drop between first and last sessions

to evaluate visual comfort of different paradigms.

Classification Accuracy Comparisons: As each trial length is 4 seconds, different window lengths from 0.5 to 4 seconds with an interval of 500 millisecond are used to perform classification and identify each trial's label. Fig. 4.3 shows the average accuracy of three stimulations simultaneously. The best accuracy (95.31%) for this experiment belongs to the square based SSmVEP when the trial time length is 4 seconds. Nevertheless, in other time windows, Flickering paradigm has the best performance among the stimuli. Square-based paradigm shows better accuracy than the circle-based paradigm over different time lengths. It is worth mentioning that it is expected at first that a normal SSVEP provides better accuracy and ITR due to its obviousness. Although in our experiments the flickering pattern provides better performance in smaller window lengths in terms of SSVEP-frequency detection and ITR, a significant reduction of accuracy between the first and last trials is observed indicating the mentioned drawbacks such as causing seizures and eye tiredness.

Information Transfer Rate of Different Paradigms: Fig. 3.5 illustrates the computed ITRs associated with three paradigms over various time windows. The highest rate of our BCI system is 39.12 bits/min, which belongs to the flickering stimulus. Square-based SSMVEP has a higher ITR than the Circle-based paradigm in all the time windows. Although flickering paradigm provides higher ITR during smaller time windows, the one (24.79 bits/minute) associated with the Square-based SSMVEP is higher when the complete trial is used (4 seconds). The relatively high achieved ITRs for the initial SSmVEP designs are encouraging to further improve the designs, which is the focus of our on-going research work.

Accuracy Drop Between First and Last Sessions: Each test round consists of two consecutive sessions and each session has four trials for each target frequency. To evaluate visual comfort of different paradigms, the summation of the second and fourth session is subtracted from the summation of the first and the third sessions. Fig. 3.6 shows the average accuracy difference between consecutive sessions. Furthermore, the range of time lengths for trials is from 0.5 to 2 seconds. Based on this comparison and according to their visual fatigue, Square-based SSMVEP, Circle-based SSMVEP, and flickering SSVEP are ranked first, second, and third, respectively. The result of this experiment illustrates potential benefits of the proposed SSMVEP paradigms in providing less visual fatigue.

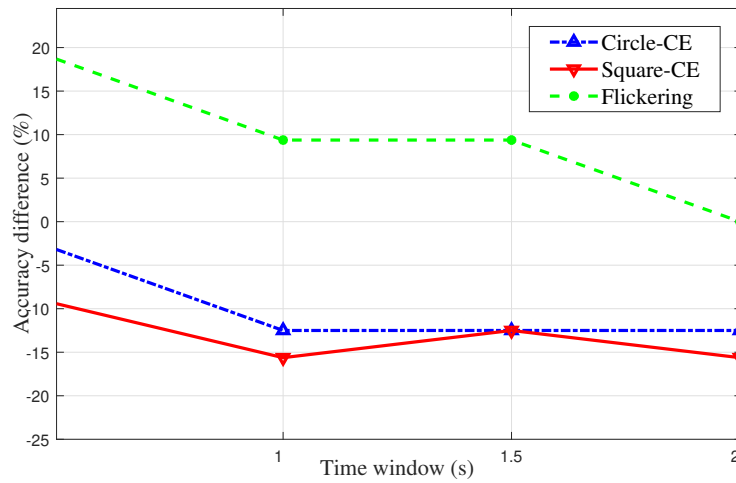


Figure 3.6: Accuracy reduction between first and last sessions.

3.4 Summary

Despite the popularity of SSVEPs, their utilization for practical applications especially for assistive technologies is complicated and challenging, which can be attributed to the following key issues: (i) Eye fatigue with low-frequency flickering, and; (ii) Higher risk of induced epileptic seizure with medium-frequency flickering. The chapter proposed two novel Steady-State Motion Visual Evoked Potentials (SSMVEP) paradigms with low luminance contrast. The key issue being targeted is fatigue of flicker (or brightness modulation) via development of two different patterns with oscillating expansion and contraction motions.

Chapter 4

DF-SSmVEP: Dual Frequency

Aggregated Steady-State Motion Visual

Evoked Potential Design with Bifold

Canonical Correlation Analysis

Recent advancements in Electroencephalography (EEG) sensor technologies and signal processing algorithms have paved the way for further evolution of Brain Computer Interfaces (BCI) in several practical applications ranging from rehabilitation systems to smart consumer technologies. When it comes to Signal Processing (SP) for BCI, there has been a surge of interest on Steady-State motion-Visual Evoked Potentials (SSmVEP), where motion stimulation is utilized to address key issues associated with conventional light-flashing/flickering. Such benefits, however, come with the price of having less accuracy and less Information Transfer Rate (ITR). In this regard, the chapter focuses on the design of a novel SSmVEP paradigm without using resources such as trial time, phase, and/or number of targets to enhance the ITR. The proposed design is based on the intuitively pleasing idea of integrating more than one motion within a single SSmVEP target stimuli, simultaneously. To elicit SSmVEP, we designed a novel and innovative dual frequency aggregated modulation paradigm, referred to as the Dual Frequency Aggregated steady-state motion Visual Evoked

Potential (DF-SSmVEP), by concurrently integrating “Radial Zoom” and “Rotation” motions in a single target without increasing the trial length. Compared to conventional SSmVEPs, the proposed DF-SSmVEP framework consists of two motion modes integrated and shown simultaneously each modulated by a specific target frequency. The chapter also develops a specific unsupervised classification model, referred to as the Bifold Canonical Correlation Analysis (BCCA), based on two motion frequencies per target. The corresponding covariance coefficients are utilized as extra features improving the classification accuracy. The proposed DF-SSmVEP is evaluated based on a real EEG dataset and the results corroborate its superiority. The proposed DF-SSmVEP outperforms its counterparts and achieved an average ITR of 30.7 ± 1.97 and an average accuracy of 92.5 ± 2.04 , while the Radial Zoom and Rotation result in average ITRs of 18.35 ± 1 and 20.52 ± 2.5 , and average accuracies of 68.12 ± 3.5 and 77.5 ± 3.5 respectively.

4.1 Introduction

Generally speaking, there are two main visual BCI Paradigms, (1) *Steady-State Visually Evoked Potential (SSVEP)* [34–40], where light-flashing (flickering) visual stimulus is used to induce evoked potentials in the EEG signals, and; (2) *Steady-State motion-Visual Evoked Potentials (SSmVEP)* [28, 41, 42, 59], where instead of using flickering, some form of graphical motion is used to evoke potentials. The former category (SSVEP) has been the main research theme due to its high achievable Information Transfer Rate (ITR), minimal requirement for user training, and excellent interactive potentials, such as high tolerance to artifacts and robust performance across users. However, flickering light, causes extensive mental stress. Continuous use of SSVEPs (looking at flickering patterns for a long period of time), therefore, may cause seizure or eye fatigue. The second category (SSmVEP) is introduced to address these issues while keeping all the aforementioned benefits of the SSVEPs.

Contributions: To address the problems mentioned in Sub-section 2.1.3, we focus on designing a novel SSmVEP paradigm without using additional resources such as trial time, phase, and/or number of targets to enhance the ITR. The proposed design is based on the intuitively pleasing idea of using more than one simultaneous motion within a single SSmVEP target stimuli. More specifically,

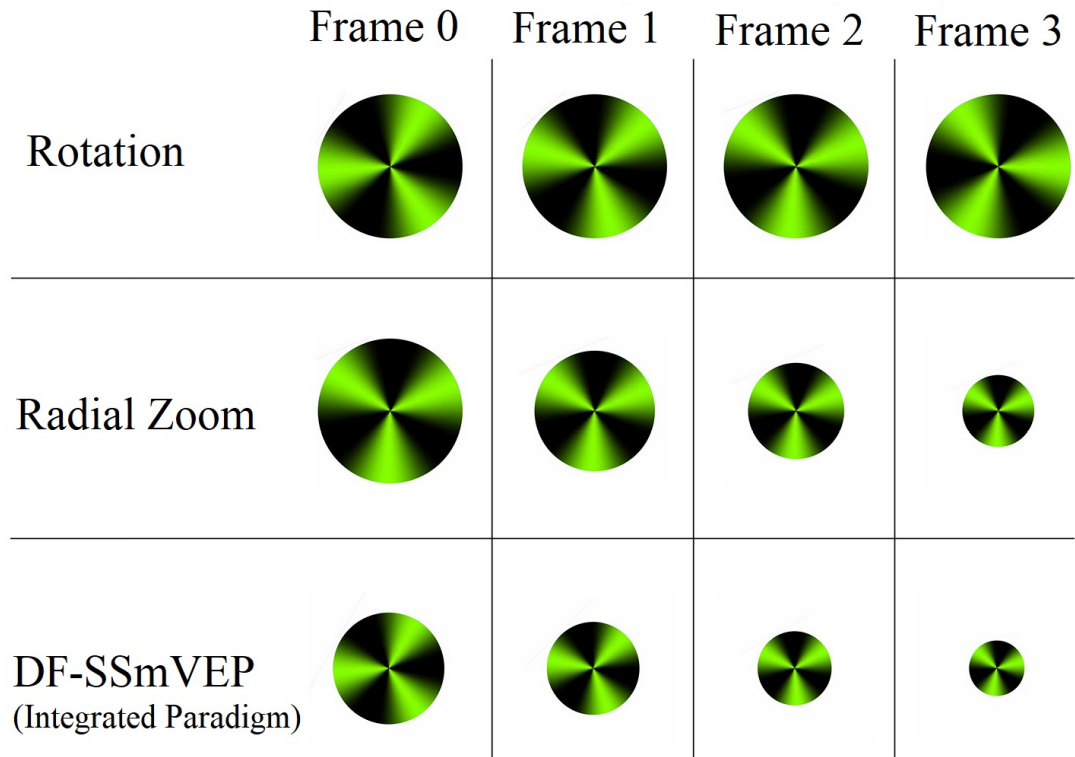


Figure 4.1: Proposed DF-SSmVEP paradigm developed by concurrent inclusion of two types of the motion (rotation and resizing).

as shown in Fig. 4.1, to elicit SSmVEP we designed a novel and innovative dual frequency aggregated modulation paradigm, referred to as the DF-SSmVEP, by concurrently integrating “Radial Zoom” and “Rotation” motions in a single target without increasing the trial length.

Fig. 4.2(i) visually compares four different paradigms: Conventional SSVEP frequency modulation is shown in Sub-figure (a), where 2 target frequencies, “F1” and “F2”, are evoked in 2 different trials via flickering. Sub-figure (b) is similar to Sub-figure (a) where now 2 target frequencies are used together, one after another by increasing the trial time. Sub-figure (c) in Fig. 4.2(i) illustrates 2 SSmVEP modulations similar to Sub-figure (a), but target frequencies are evoked now via motion of the circle. Sub-figure (d) shows the proposed DF-SSmVEP design where now 2 target frequencies are used together simultaneously eliminating the need to increase (sacrifice) the trial length for achieving higher accuracy as is the case in code/frequency modulated SSVEPs [35–37]. It is

worth mentioning that the proposed idea has not been considered previously as the main focus of the literature was on SSVEPs using flickering frequencies, where it is impossible to implement our intuitive idea of having two target motion frequencies embedded in a single target, simultaneously.

The chapter also develops a specific unsupervised classification model adopted to the proposed innovative DF-SSmVEP paradigm. More specifically, in contrary to the existing works, we propose an unsupervised SSmVEP detection technique, referred to as the Bifold Canonical Correlation Analysis (BCCA) utilizing unique characteristics of the proposed dual aggregated frequency design. The BCCA exploits availability of two motion frequencies for each target and separately considers each single frequency of the targets as a reference. The corresponding covariance coefficients are then used as extra features advancing the classification accuracy. The proposed DF-SSmVEP is evaluated based on a real EEG dataset.

4.2 The Proposed DF-SSmVEP

The designed DF-SSmVEP stimulation paradigm includes a green and black circle with two motion modes. The first motion is the “Radial Zoom” in which the size of the circle changes periodically. The second mode is the “Reciprocal Rotation” of the circle between -45° and 75° . Radial zoom motion and rotation motion are selected as candidates for integration following previous evaluations [28, 44]. The frequency of motion direction change inside the reciprocal motion is defined as motion inversion frequency. Furthermore, the motion inversion frequency corresponds to the frequency of stimulation, which is equal to the fundamental SSmVEP frequency. To elaborate on the motion choices utilized to design the proposed DF-SSmVEP paradigm, first we note that as mentioned in [44], any paradigms with periodic motion can be used as stimuli of SSmVEPs.

The two designs are integrated such that the focal point of one paradigm is overlaid with that of the second one. In the proposed DF-SSmVEP paradigm, the focal point will be the center of the black-green circle, i.e., the center of oscillation for the two segments of the design (resizing and oscillation of circle). To make the proposed design as efficient as possible and to reduce fatigue [45], the proposed DF-SSmVEP design does not include high contrast colors improving the practical applicability of the SSmVEP stimuli. As shown in Fig. 4.2(b), the Luminance Contrast Ratio (LCR)

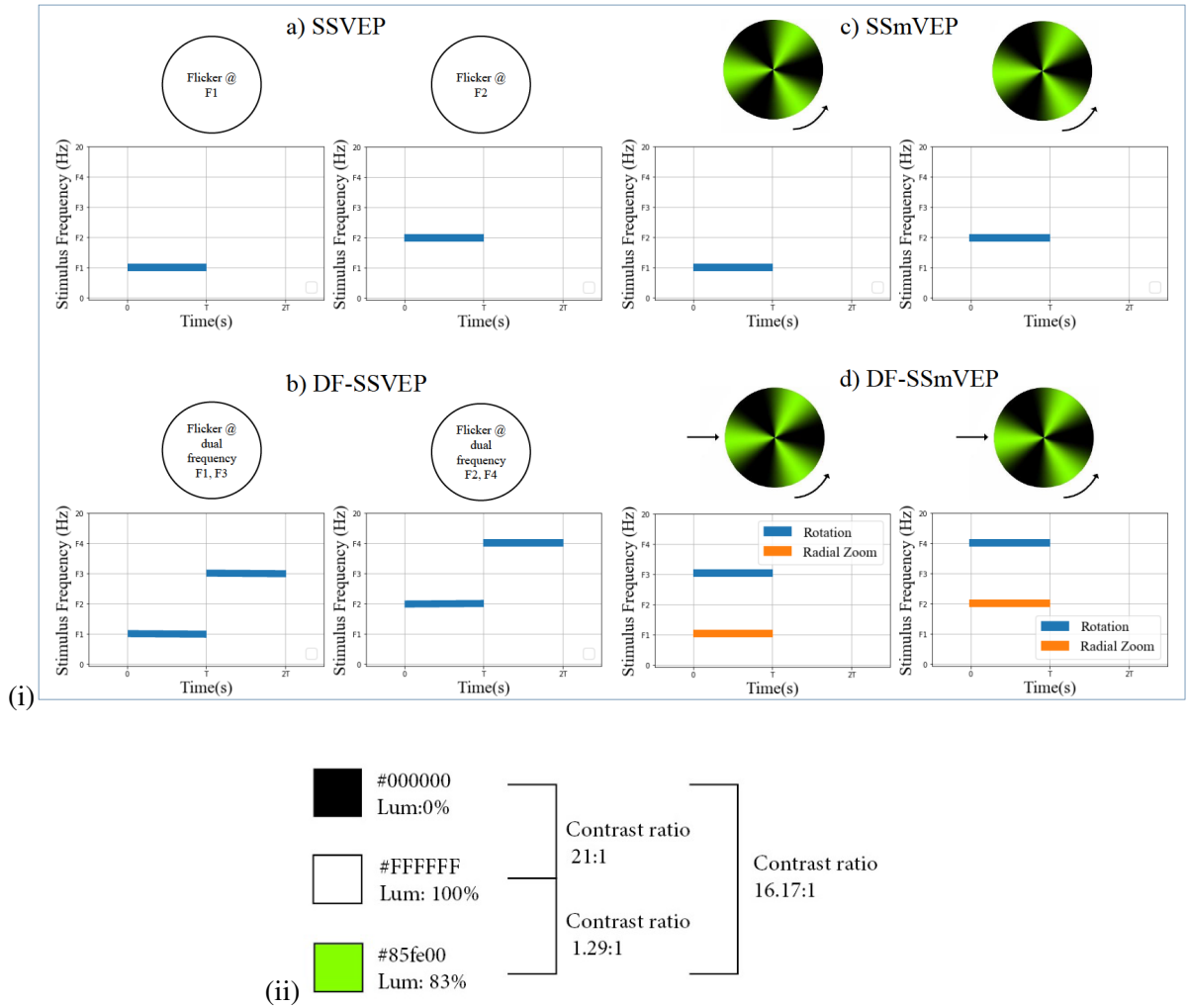


Figure 4.2: (i) Comparison between existing SSVEP frequency modulation schemes ((a) and (b)) with SSmVEP (c), and the proposed DF-SSmVEP (d). (ii) Luminance contrast ratio of the colors used in the designed DF-SSmVEP.

associated with our green-black paradigm is lower than that of the conventional black-white design.

The refresh rate of the monitor showing the SSmVEP stimuli is a limiting factor restricting the frequencies that can be designed when an equal number of frames used during consecutive cycles (one motion direction change). To implement flexible target frequencies, we need to have designs with variable number of frames per cycle [45] to implement our design. Given the refresh rate of the monitor, which is 60 Hz in our setting, the first task is to design binary stimulus sequences (i.e., the number of frames per each half-cycle, typically, asymmetric) with the goal of allocating

frames based on the specified target frequencies. The number of frames per half-cycle [45] of the DF-SSmVEP is constructed as $S(f^{(T)}, i) = \text{square}[2\pi f^{(T)}(\frac{i}{R_r})]$, where i indicates the frame index; f denotes the target frequency; R_r represents the monitor's refresh rate, and; $S(f, i)$ denotes the stimulus sequences associated with target frequency f . Note that, each half-cycle corresponds to one contraction or expansion or half of the reciprocal motion. Consequently, a motion oscillation at a target SSmVEP frequency up to $f \leq R_r/k$ can be generated as a stimulus. In other words, for one cycle of an SSmVEP paradigm to be understandable, k minimum number of frames per half-cycle is required to realize the motion cycle comfortably.

Coding Algorithm: Assume that the maximum number of targets (objects shown on the screen simultaneously) is denoted by $N^{(T)}$. In other words, $N^{(T)}$ number of target frequencies are selected within the limited frequency spectrum of $[f_{\min}, f_{\max}]$ available for constructing the stimuli. Term f_i , for $(1 \leq i \leq N^{(T)})$, represents the target frequency for the i^{th} target/object assumed to be sorted in an ascending order, i.e., $(f_{\min} \leq f_1 < f_2 < \dots < f_{N^{(T)}} \leq f_{\max})$. These $N^{(T)}$ target frequencies need to be derived in an intelligent fashion such that the best performance among all the susceptible frequencies is achieved (i.e., achieve accuracy improvements without reducing the ITR). *In the proposed dual aggregated design, each target includes two motions with two distinct frequencies.* These frequencies are assigned to targets in which no two pairs of targets have more than one adjacent frequencies. More specifically, the objective of the coding algorithm is to find these two underlying target frequencies in such a way that each pair of objects at most have one adjacent target frequency. For each consecutive frequencies f_i and f_{i+1} , g_i is defined as

$$g_i = \begin{cases} \frac{f_i + f_{i+1}}{2}, & \forall i \in [1, N - 1] \\ f_i + M, & i = N \end{cases} \quad (4.1)$$

where $M = \min[\frac{f_{i+1} - f_i}{2}] \forall i \in [1, N - 1]$. Each g_i is adjacent to f_i and f_{i+1} . More specifically, consider $P = \{(a_i, b_i)\}$, for $(1 \leq i \leq N)$, representing the set of $N \geq 5$ target pairs where a_i and b_i are the new SSmVEP frequencies used for the i^{th} object. Terms a_i and b_i in P are defined as

follows

$$a_i = \begin{cases} f_1, & i = 1 \\ f_{i+1}, & \forall i \in [2, N-1] \\ f_2, & i = N \end{cases} \quad b_i = \begin{cases} g_{N-1}, & i = 1 \\ g_{i-1}, & \forall i \in [2, N-1] \\ g_N, & i = N \end{cases} . \quad (4.2)$$

Pre-processing: The proposed SSmVEP paradigm is implemented via a BCI system for real EEG data collection. In this regard, the first step is pre-processing of EEG signals associated with the proposed SSmVEP paradigm, as collected EEG signals are exposed to artifacts and high/low frequency noises. To extract the SSmVEP signal from the EEG signals, applying spatial and time domain filters are, therefore, critical. In time domain filtering, first, zero-phase Chebyshev Type I band-pass filter (2-40 Hz) is applied to smooth the data and remove high-frequency artifacts.

4.2.1 Proposed BCCA Paradigm

Canonical Correlation Analysis (CCA) is a statistical method to study the linear relationship between two groups of multi-dimensional variables. For two sets of signals arranged in matrices denoted by \mathbf{X} and \mathbf{Y} , the goal is to find two linear projection vectors \mathbf{w}_x and \mathbf{w}_y , such that the linear combination of two groups of signals $\mathbf{w}_x^T \mathbf{X}$ and $\mathbf{w}_y^T \mathbf{Y}$ has the largest correlation coefficient, i.e.,

$$\rho = \max \frac{E(\mathbf{w}_x^T \mathbf{X} \mathbf{Y}^T \mathbf{w}_y)}{\sqrt{E(\mathbf{w}_x^T \mathbf{X} \mathbf{Y}^T \mathbf{w}_x) E(\mathbf{w}_y^T \mathbf{X} \mathbf{Y}^T \mathbf{w}_y)}} . \quad (4.3)$$

Reference signals are constructed at the stimulation frequency f_i as

$$\mathbf{y}_i = [\cos 2\pi f_i t, \sin 2\pi f_i t, \dots, \cos 2\pi N_h f_i t, \sin 2\pi N_h f_i t]^T, \quad (4.4)$$

where $t = \frac{1}{f_s}, \dots, \frac{m}{f_s}$, the f_s is the sampling rate, m is sample point, and N_h is the number of harmonics, which is dependent on the paradigm and is obtained experimentally from Welch Power Spectrum of signals. Consider \mathbf{X} as the matrix of the EEG signals collected from K different channels. The CCA finds linear combination of coefficients with the largest correlation between \mathbf{X} and \mathbf{Y} . In the BCCA fusion, there is a feature vector for each sample concerning each target frequency. Contemplating the Power Spectral Density (PSD) of the EEG signal, collected during the

aggregated paradigm, gives insight that only one of the peaks is significant for some trials, i.e., one of the two modulated frequencies has more impact on the visual pathways of the brain. To capitalize this unique property and enhance the DF-SSmVEP, the following three references are incorporated to create the feature vector

$$\mathbf{y}_1 = [\cos(2\pi f_{i,1}t), \sin(2\pi f_{i,1}t), \dots, \cos(2\pi N_h f_{i,1}t), \sin(2\pi N_h f_{i,1}t)]^T \quad (4.5)$$

$$\mathbf{y}_2 = [\cos(2\pi f_{i,2}t), \sin(2\pi f_{i,2}t), \dots, \cos(2\pi N_h f_{i,2}t), \sin(2\pi N_h f_{i,2}t)]^T \quad (4.6)$$

$$\mathbf{y}_c = C(\mathbf{y}_1, \mathbf{y}_2, [\cos(2\pi(f_{i,1} + f_{i,2})t), \sin(2\pi(f_{i,1} + f_{i,2})t)]^T, 2) \quad (4.7)$$

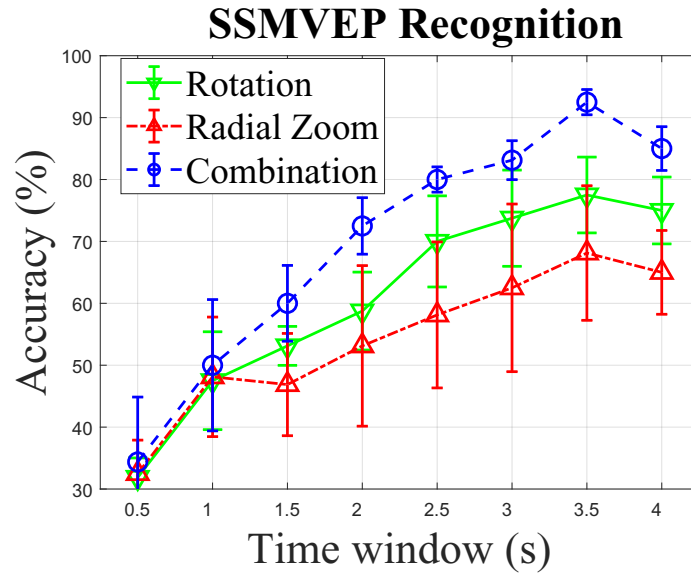
where $f_{i,j}$ represents the j^{th} stimulation frequency of i^{th} target, and the operator $C(a, b, c, 2)$ concatenates three matrices a, b, and c vertically. The projection of each vector is separately calculated leading to three different weight vectors between test signal \mathbf{X} and: (i) (w_{y_1}, w_{X_1}) sine/cosine reference of first frequencies; (ii) (w_{y_2}, w_{X_2}) reference of second frequency of targets, and; (iii) (w_{y_c}, w_{X_c}) sine/cosine reference of both frequencies of targets. The feature vector \mathbf{v} is

$$\mathbf{v} = [\rho_1, \rho_2, \rho_c]^T, \text{ and } \rho_a = \frac{\rho_1 + \rho_2 + \rho_c}{3}, \quad (4.8)$$

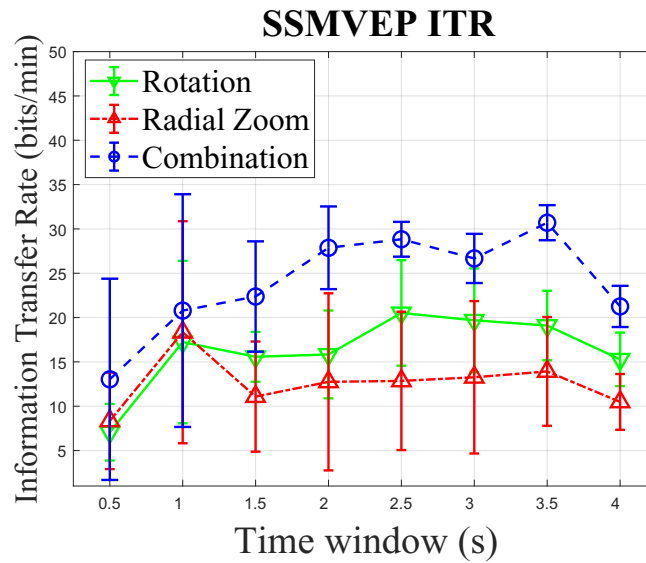
where ρ_a is used as the final value to represent the correlation between the unknown sample and the frequencies of a target. It is worth mentioning that the proposed BCCA is an unsupervised technique as such there is no need for a separate training step. Consequently, all the available trials of sessions are used in the testing stage.

4.2.2 Experimental Setup

A real dataset consisting of 10 individuals, 5 women and 5 men between age of 20 to 27 is utilized to evaluate the proposed DF-SSmVEP framework. Participants have no evidence of visual or color-recognition ailments. Five subjects had experience of BCI experiments. We would like to mention that, for data collection, we have followed the common, standard, and accepted approach in the BCI domain (e.g., [44]) where, typically 9-11 subjects are used, and the trial length ranges from



(a)



(b)

Figure 4.3: Mean and standard deviation across all subjects for each time window: (a) Accuracy comparisons. (b) ITR comparisons.

2 seconds to 6 seconds. The EEG signals were collected using a portable and wireless bio-signal acquisition system (32 bipolar active wet electrodes with sampling rate 500Hz), g.Nautilus from g.tech Medical Engineering. The reference and the ground electrodes of the headset were placed at the earlobe and frontal position (Fpz), respectively. The electrodes P_z , P_{o7} , P_{o3} , P_{o4} , P_{o8} , and O_z from the parietal-occipital region were chosen to collect EEG signals. Stimuli with a white

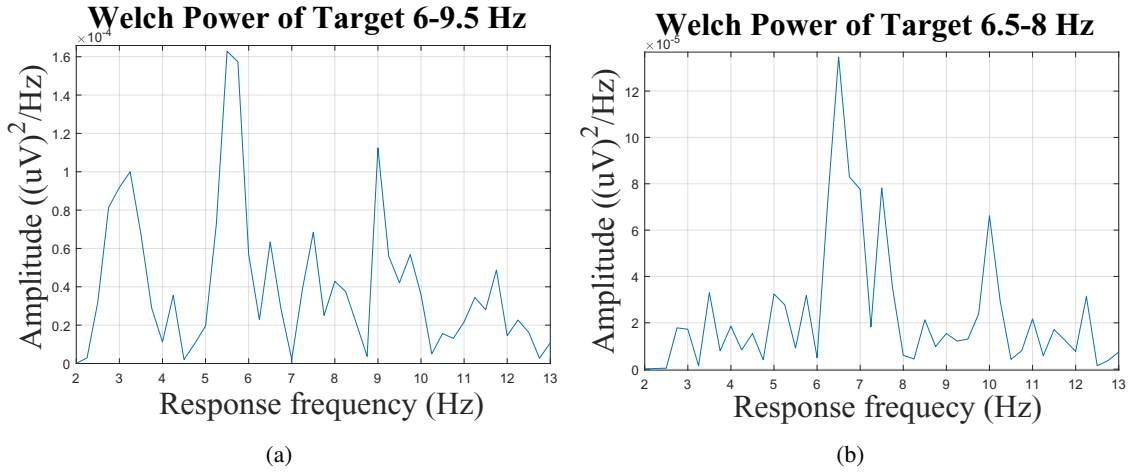


Figure 4.4: (a) The PSD plot based on aggregated SSmVEP with 6-9.5Hz target frequencies. (b) Similar to (a) but with 8-6.5Hz target frequencies.

Filters \ Paradigms	Radial Zoom		Rotation		DF-SSmVEP	
	ACC	ITR	ACC	ITR	ACC	ITR
MCF + CCA	68.12	18.35	77.5	20.52	81.88	21.89
T-F Image Fusion + CCA	59.3	13.39	68.75	13.73	63.25	13.93
CCA Fusion	63.5	17.24	76.17	18.05	84.38	23.73
BCCA Fusion	-	-	-	-	92.5	30.7

Table 4.1: Mean accuracy (%) and mean ITR (bits/min) comparison between four methods of spatial filtering across the three motions. The best ITR among different time-windows are reported for each filter. Maximum Contrast Fusion (MCF) [44] and T-F Image Fusion [42] are two types of spatial filtering.

background were displayed on a 21.5-inch LED screen at 60Hz refresh rate. The resolution of the screen was 1920×1080 , and the viewing distance was 70cm. The data were collected with the policy certification number 3007997 of Ethical acceptability for research involving human subjects approved by Concordia University.

Three paradigms, i.e., (i) Rotation; (ii) Radial zoom, and; (iii) DF-SSmVEP, are tested in separated runs (videos are available publicly at [47]). Each video consists of five targets oscillating with different frequencies. For individual videos, target frequencies were 5, 6, 7, 8, and 9Hz. For aggregated videos, target frequencies of the radial zoom pattern were 5, 6, 7, 8, and 9Hz, and target frequencies of the rotation pattern were 5.5, 6.5, 7.5, 8.5, and 9.5Hz. Each run of a video included

Table 4.2: Comparison between mean and standard deviation values associated with performance indices (precision, sensitivity, specificity, and accuracy across) all runs for 3 paradigms, i.e., Rotation (R), Radial Zoom (RZ), and the proposed DF-SSmVEP (denoted by DF).

Classes \ PI	Specificity			Sensitivity		
	R	RZ	DF	R	RZ	DF
9 Hz or (9Hz, 7.5Hz)	0.912 ± 0.052	0.934 ± 0.037	0.993 ± 0.013	0.900 ± 0.098	0.600 ± 0.226	0.875 ± 0.083
6 Hz or (6Hz, 9.5Hz)	0.940 ± 0.023	0.893 ± 0.062	0.984 ± 0.027	0.725 ± 0.098	0.875 ± 0	0.962 ± 0.060
5 Hz or (5Hz, 8.5Hz)	0.946 ± 0.025	0.875 ± 0.044	0.940 ± 0.033	0.625 ± 0.220	0.937 ± 0.106	0.975 ± 0.053
7 Hz or (7Hz, 5.5Hz)	0.981 ± 0.030	0.993 ± 0.013	0.993 ± 0.013	0.787 ± 0.177	0.312 ± 0.135	1 ± 0
8 Hz or (8Hz, 6.5Hz)	0.940 ± 0.047	0.906 ± 0.062	0.987 ± 0.016	0.850 ± 0.098	0.687 ± 0.244	0.812 ± 0.135

Classes \ PI	Precision			Accuracy		
	R	RZ	DF	R	RZ	DF
9 Hz or (9Hz, 7.5Hz)	0.735 ± 0.137	0.710 ± 0.061	0.977 ± 0.047	0.910 ± 0.054	0.867 ± 0.020	0.970 ± 0.01
6 Hz or (6Hz, 9.5Hz)	0.757 ± 0.091	0.702 ± 0.167	0.947 ± 0.870	0.897 ± 0.027	0.890 ± 0.050	0.980 ± 0.023
5 Hz or (5Hz, 8.5Hz)	0.737 ± 0.118	0.663 ± 0.068	0.829 ± 0.100	0.882 ± 0.054	0.8875 ± 0.017	0.952 ± 0.029
7 Hz or (7Hz, 5.5Hz)	0.937 ± 0.100	0.933 ± 0.140	0.977 ± 0.047	0.942 ± 0.026	0.857 ± 0.031	0.995 ± 0.011
8 Hz or (8Hz, 6.5Hz)	0.809 ± 0.131	0.649 ± 0.221	0.939 ± 0.079	0.922 ± 0.027	0.862 ± 0.095	0.952 ± 0.036

two consecutive sessions, where subjects were required to stare at a target using a pointer. In each session, each existing target was pointed in four trials. Each trial lasted 3.5 seconds with a 2.5 seconds break between consecutive trials. In particular, ITR is used for evaluations, which assesses the speed of a BCI systems as

$$ITR = \frac{60}{T} \left[\log_2 K + \sigma \log_2 \sigma + (1 - \sigma) \log_2 \left(\frac{1 - \sigma}{K - 1} \right) \right], \quad (4.9)$$

where T is the sum of time of each trial and the resting state time between two trials; K is the number of stimuli, and; σ is the recognition accuracy. Evaluation via the One-way Analysis Of Variance (ANOVA) [46] with Tukey post hoc analysis is also used to confirm that responses to the proposed DF-SSmVEP-stimuli is statistically meaningful ($p < 0.05$).

4.3 Result

As shown in Fig. 4.3, accuracy and ITR are measured for different time windows for each trial ranging from 0.5 to 4 seconds with an interval of 500 millisecond. The highest rate of transmission (ITR) belongs to aggregated motion (30.7 ± 1.97), which also achieved the best accuracy (92.5 ± 2.04). We utilized the ANOVA test following the existing literature [44, 59] that used ANOVA test for significance comparison between accuracies and/or ITRs of different paradigms. It is worth noting that based on the Central Limit Theorem, we can safely assume that the samples have a normal distribution. The one-way ANOVA on accuracies of DF-SSmVEP paradigm reveals that there is no significant effect of frequencies (classes) on accuracies ($F = 2.78$, $p = 0.065$), so all target frequencies of DF-SSmVEP are feasible in BCI systems. The Tukey post-hoc test on the accuracy and the ITR shows significant differences between the performance of DF-SSmVEP with BCCA and other paradigms with corresponding classifiers for which the highest accuracies are acquired, i.e., (Accuracy: $p_{DF-R} = 0.042$, $p_{DF-RZ} = 0.002$, $p_{R-RZ} = 0.218$; ITR: $p_{DF-R} = 0.011$, $p_{DF-RZ} = 0.001$, $p_{R-RZ} = 0.264$). The second best motion in terms of accuracy is the rotation 77.5 ± 6.12 , and the last one is radial zoom (68.12 ± 10.87).

Fig. 4.4 illustrates Welch PSD of two targets of aggregated motion after spatial filtering for Subject 1. Two significant peaks of SSmVEP frequency around the two frequencies of each target is observable. Table 4.2.2 shows the overall recognition accuracies and ITRs. It can be observed that aggregating two SSmVEP paradigms using the proposed DF-SSmVEP results in compelling performance improvement. The results also show superiority of the BCCA as the best unsupervised target detector among its counterparts. Means and standard deviations based on four different Performance Indices (PI), i.e., precision, sensitivity, specificity, and accuracy across all runs for each

class, are also shown in Table 4.2. The time window is set to 3.5 second. Each row of Table 4.2 corresponds to the dual frequency of the proposed DF-SSmVEP paradigm in each class. To investigate robustness of the proposed methodology, we display paradigms repeatedly to different subjects (in contrary to using EEG signals of one trial several times) and average the performance across Runs and Subjects. In the experiments, we have 10 subjects each performing (repeating) one run for 8 times (resulting in 80 trials per class).

4.4 Summary

To address lower accuracy and ITR of SSmVEP designs, the chapter proposed an intuitively pleasing, novel, and innovative dual frequency aggregated modulation paradigm. Referred to as the DF-SSmVEP, the novel design is constructed by concurrently integrating “Radial Zoom” and “Rotation” motions in a single target without increasing the trial length. The chapter also develops a specific unsupervised classification model, referred to as the BCCA, which utilizes availability of two motion frequencies per each target. The proposed DF-SSmVEP is evaluated via a real EEG dataset achieving average ITR of 30.07 ± 1.97 and average accuracy of 92.5 ± 2.04 .

Chapter 5

Deep Video Canonical Correlation

Analysis for Steady State motion Visual

Evoked Potential Feature Extraction

5.1 Introduction

As stated previously, there has been a surge of interest in development of BCI systems based on SSmVEP, where motion stimulation is utilized to address high brightness and uncomfortably issues associated with conventional light-flashing/flickering. In this chapter, we propose a deep learning-based classification model that extracts features of the SSmVEPs directly from the videos of stimuli. More specifically, the proposed deep architecture, referred to as the Deep Video Canonical Correlation Analysis (DvCCA), consists of a Video Feature Extractor (VFE) layer that uses characteristics of videos utilized for SSmVEP stimulation to fit the template EEG signals of each individual, independently. The proposed VFE layer extracts features that are more correlated with the stimulation video signal as such eliminates problems, typically, associated with deep networks such as overfitting and lack of availability of sufficient training data. The proposed DvCCA is evaluated based on a real EEG dataset and the results corroborate its superiority against recently proposed state-of-the-art deep models.

The chapter is motivated by the desire for having a classification model that can extract all the features of the SSmVEPs, mentioned in Sub-section 2.1.4, directly from the videos of stimuli. In this regard, we propose an intuitively pleasing deep learning-based classification model, referred to as the Deep Video Canonical Correlation Analysis (DvCCA), which consists of a Video Feature Extractor (VFE) layer that uses characteristics of videos utilized for SSmVEP stimulation to fit the template EEG signals of each individual, independently. The proposed VFE layer extracts features that are more correlated with the stimulation video signal as such eliminates problems, typically, associated with deep networks such as overfitting and lack of availability of sufficient training data. Moreover, in comparison to other deep networks, the proposed DvCCA architecture uses the extra information of videos, therefore, requiring less training data, which is critical for BCI systems having available few template samples of the subjects.

5.2 Methods and Materials

5.2.1 Stimulation Design

To achieve the objectives outlined in Section 5.1, four novel SSmVEP based paradigms with four motion modes shown in Fig. 5.1 are designed. The first mode (Fig. 5.1(a)) is the “Reciprocal Rotation” of a green and black circle between -45° and 75° . The second motion (Fig. 5.1(b)) is the “Radial Zoom” in which the size of a green and black circle changes periodically. The third mode (Fig. 5.1(c)) is “Swing” centering around the middle of a black line. Finally, the last motion (Fig. 5.1(d)) is the “Sway” of a green rectangular centering around the width. The frequency of motion direction change inside the reciprocal motion is defined as motion inversion frequency. The motion inversion frequency corresponds to the frequency of stimulation, which is equal to fundamental SSmVEP frequency in the EEG signals.

To elaborate on the motion choices utilized in our designs, we note that as mentioned in Reference [44], any paradigm with periodic motion can be used as stimuli of SSmVEPs. Each designed SSmVEP paradigm has a focal point where the paradigm oscillates/moves around this fixed center-point. Other factors that play crucial roles in our designs are brightness and luminance-contrast of the colors used in the paradigm. To make the proposed designs as efficient as possible, we capitalize

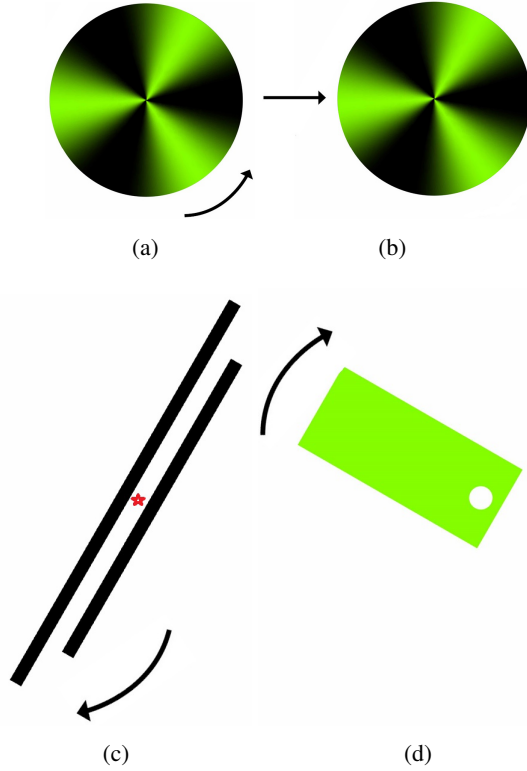


Figure 5.1: The four designed SSmVEP paradigms: (a) Reciprocal-Rotation; (b) Radial-Zoom; (c) Swing; (d) Sway.

on previous works [64] performed to investigate effects of different SSmVEP patterns with different brightness on accuracy and fatigue.

The refresh rate of the monitor showing the SSmVEP stimuli is a limiting factor restricting the frequencies that can be designed when an equal number of frames are used during consecutive cycles (one motion direction change). To implement flexible target frequencies, we need to have designs with variable number of frames per cycle; as such, we used the technique in Reference [45] and verified in [76] to implement our designs. Given the refresh rate of the monitor, the first task is to design binary stimulus sequences (i.e., the number of frames per each half-cycle, typically, asymmetric) with the goal of allocating frames based on the specified target frequencies. Following Reference [45], the number of frames per half-cycle of our paradigms are constructed as follows

$$S(f, i) = \text{square}\left[2\pi f\left(\frac{i}{R_r}\right)\right], \quad (5.1)$$

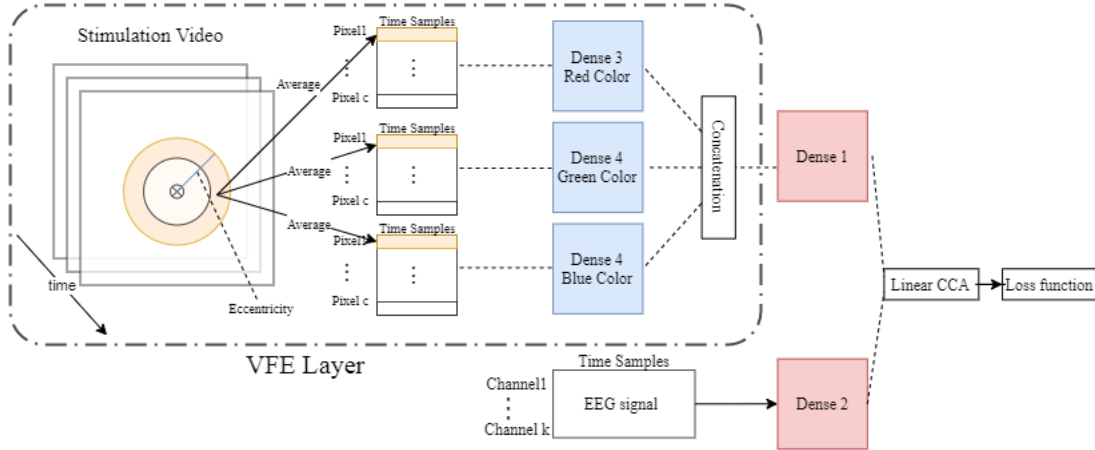


Figure 5.2: Architecture of the proposed Deep Video Canonical Correlation Analysis (DvCCA). where i indicates the frame index; f denotes the target frequency; R_r represents the monitor’s refresh rate, and; $S(f, i)$ denotes the stimulus sequences associated with target frequency f . Note that, each half-cycle corresponds to one contraction or expansion or half of the reciprocal motion. Consequently, a motion oscillation at a target SSmVEP frequency up to $f \leq R_r/k$ can be generated as a stimulus. In other words, for one cycle of an SSmVEP paradigm to be understandable, k minimum number of frames per half-cycle is required for the subject to realize the motion cycle comfortably. The proposed SSmVEP paradigms are displayed as stimulations for EEG data collection. The first step is pre-processing of the EEG signals as they are, typically, exposed to artifacts and high/low frequency noises. To extract the SSmVEP from the EEG signals, applying spatial and time domain filters are, therefore, necessary. In time domain filtering, first, zero-phase Chebyshev Type I band-pass filter (2-40 Hz) is applied to smooth the data and remove high-frequency artifacts.

5.3 Deep Video Canonical Correlation Analysis (DvCCA)

5.3.1 Initial Weight Extraction from Videos

The proposed DvCCA model is developed based on the following facts: (1) Changing color of each pixel in the stimulation video can evoke EEG signals; (ii) Harmonic frequencies of the signal of each pixel across time can appear in the EEG data depending on the distance of the pixel from the focal point of the target, and; (iii) The final visual evoked potential consists of the impact of

the time signal of all the pixels. Therefore, the visual field incorporating the distance between the subject and the monitor and location of two pixels in the image is a suitable criterion to measure the mentioned distance in this context. The visual field (in degree) between the focal point and any arbitrary pixel is called eccentricity [57]. The more eccentricity of each pixel is from the focal point, the more trivial the trace of the time signal of the corresponding pixel will be in the VEP. Therefore, the first layer of the one side of our network tries to translate, via a dense layer, time series of different pixels to come up with a new representation for SSmVEP signal. The eccentricity of each pixel will be used for weight assignment in this layer.

5.3.2 The DvCCA Network Architecture

Architecture of the proposed DvCCA is shown in Fig. 5.2. The network has two segments consisting of 3 layers of dense neural networks. The objective is to project two datasets \mathbf{X} , and \mathbf{Y} to a new space where the linear CCA is compatible to the types of the two dataset. Matrix $\mathbf{X} \in \mathbb{R}^{K \times m}$ represents the EEG time samples from K channels and is the input of the first segment. Matrix $\mathbf{Y} \in \mathbb{R}^{3f \times m}$, where m denotes number of time sample, and $3f$ denotes the output size of the Video Feature Extractor (VFE) layer, is the input of the second segment and output of the VEP layer. The propagation rule of each segment with input $\mathbf{X} \in \mathbb{R}^n$ is defined as follows

$$\mathbf{H}^{(i+1)} = \sigma(\mathbf{W}^X \mathbf{H}^{(i)} + \mathbf{b}^X), \quad (5.2)$$

where $\mathbf{W}^X \in \mathbb{R}^{n_i \times n_{i+1}}$ is a matrix of weights, $\mathbf{b}^X \in \mathbb{R}^{n_{i+1}}$, is a bias vector, H_i is the representation of data, and n_i is the number of nodes at i^{th} layer, and σ is Rectified Linear Unit (ReLU). The ultimate loss function is the linear CCA between output layers of the two segments. Adam optimizer is utilized for performing the optimization task.

Video Feature Extractor (VFE) Layer, is a dense layer in which the input is the video of stimulus with frame size $a \times b$ after applying sinc interpolation in time domain, and the output is time features associated with the video for each of the three RGB color channels. The time signals corresponding to pixels with identical distance to the focal point are averaged to generate a new tensor $\mathbf{Z} \in \mathbb{R}^{c \times m \times 3}$, where c is the number of groups of pixels. Each of the three RGB color

channels, is provided separately to a different dense network and the outputs are concatenated. The input of the network is $\mathbf{Z}_i \in \mathbb{R}^c$ at the i^{th} time sample, and output of each dense network is

$$\text{output} = \sigma(\mathbf{W}^Z \mathbf{Z}_i + \mathbf{b}^Z), \quad (5.3)$$

where $\mathbf{W}^Z \in \mathbb{R}^{c \times f}$ is a matrix of weights, and $\mathbf{b}^Z \in \mathbb{R}^f$, is a bias vector. The learnable variables of the network are measured via back propagation of CCA loss function.

User Specific Training Procedure: For each subject, the method is fitted individually and the network is validated on the template data of the same participant. Moreover, we perform 8-Fold cross-validation to test the proposed DvCCA classifier. Each trial is divided into 8 equal segments and the algorithm is performed for different window lengths obtained from these segments.

Performance Evaluation: Classification accuracy and ITR evaluate the performance of the paradigms. The ITR is a valid criterion to assess the speed of BCI systems and is computed as

$$\text{ITR} = \frac{60}{T} \left[\log_2 K + \sigma \log_2 \sigma + (1 - \sigma) \log_2 \left(\frac{1 - \sigma}{K - 1} \right) \right], \quad (5.4)$$

where T is the sum of time of each trial and the resting state time between two trials, K is the number of stimuli, and σ is the recognition accuracy. Additionally, the accuracy-difference between trials of two consecutive sessions can be used as an effective assessment to measure the fatigue associated with a designed paradigm. Evaluation of SSmVEP performance via the one-way analysis of variance (ANOVA) is a renowned metric, therefore, ANOVA is run to guarantee that the subject's response to the SSmVEP-stimuli are statistically meaningful. The statistical significance was defined as $p < 0.05$.

5.4 Experimental Results

5.4.1 Experimental Setup

In this section, we evaluate the proposed DvCCA based on a real dataset consisting of 10 individuals, 5 women and 5 men between age of 20 to 27. Participants have no evidence of visual

or color-recognition ailments. Five subjects had experience of BCI experiments. The EEG signals were collected using a portable and wireless bio-signal acquisition system (32 bipolar active wet electrodes with sampling rate 500Hz), g.Nautilus from g.tech Medical Engineering. The reference and the ground electrodes of the headset were placed at the earlobe and frontal position (Fpz), respectively. The electrodes P_z , P_{o7} , P_{o3} , P_{o4} , P_{o8} , and O_z from the parietal-occipital region were chosen to collect EEG signals. Stimuli with a white background were displayed on a 21.5-inch LED screen at 60Hz refresh rate. The resolution of the screen was 1920×1080 , and the viewing distance was 70cm. The data were collected with the policy certification number 3007997 of Ethical acceptability for research involving human subjects approved by Concordia University.

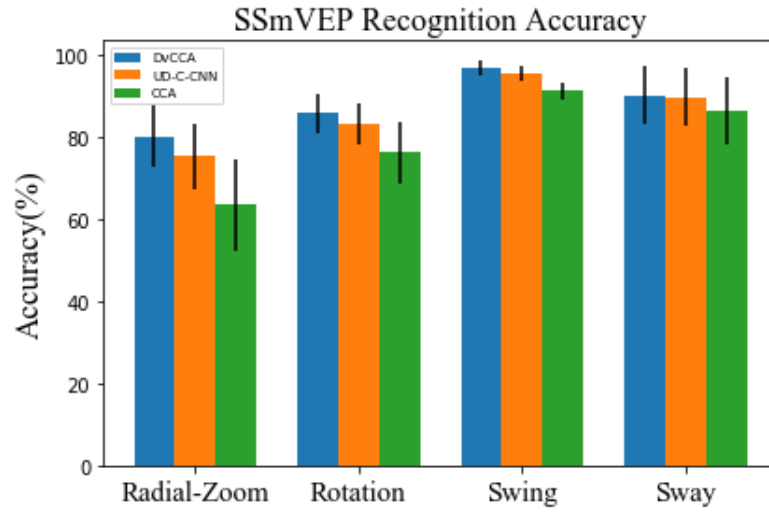
The size of the VFE layer is set to 10 in our experiments. The Learning Rate, Epoch Number, and Mini batch size are set to 10^{-3} , 50, and 100, respectively. The regularization parameter is set to 10^{-5} to avoid gradient exploding.

5.4.2 Experimental Protocol

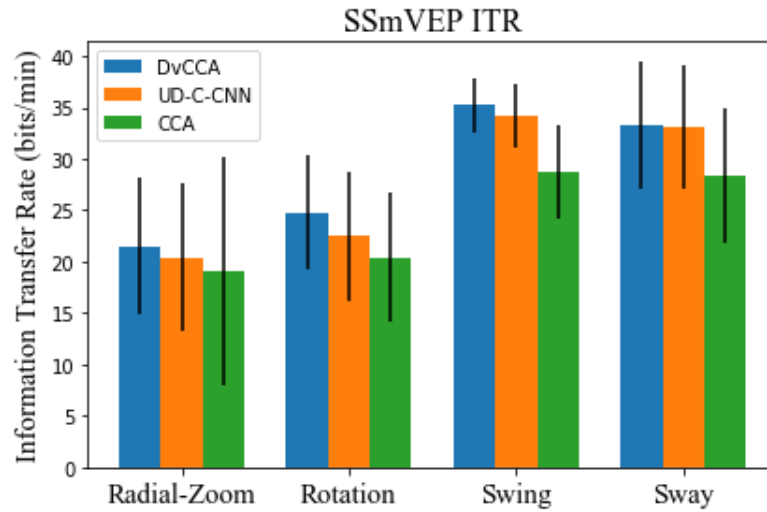
Four paradigms, i.e., (i) Rotation; (ii) Radial zoom, and; (iii) Swing; (v) Sway, are experimented in separate runs. The target frequencies were 5, 6, 7, 8, and 9Hz and subjects are asked to focus on the focal point. Each run of a video included two consecutive sessions. Subjects were required to stare at a target using a pointer. In each session, each existing target is pointed in four trials. Each trial lasted 3.5 seconds with a 2.5 seconds break between consecutive trials and 10 minutes break between two runs.

5.4.3 Result

The proposed DvCCA is applied to the data of each subject separately. A recently proposed technique, the UD-C-CNN with the configuration introduced in Reference [74], is applied to our dataset for comparison purposes. More specifically, comparisons are performed between UD-C-CNN method, regular CCA, and the proposed DvCCA method. The target detection is done for eight time windows and the best results among time windows are represented in the diagrams.



(a)



(b)

Figure 5.3: Comparison of accuracy and Information Transfer Rate (ITR) across four different SSmVEP paradigms: (a) Mean and standard deviation of SSmVEP recognition accuracy comparisons. (b) ITR of different target identification methods across the 10 subjects.

Accuracy Comparisons

Fig. 5.3(a) evaluates performance in terms of the mean and standard accuracy across subjects. It can be observed that the proposed DvCCA outperforms its counterparts across all the tested paradigms. The DvCCA results in the accuracy of 80.1 ± 7.5 , 85.8 ± 4.7 , 96.8 ± 1.7 , and $90.1 \pm 7.1\%$ for the Radial-Zoom, Reciprocal Rotation, Swing, and Sway paradigms, respectively. The swing

paradigm has the best accuracy with one-way ANOVA showing statistical significance ($F = 5.72$, $p = 0.015$).

ITR Comparisons

Fig. 5.3(b) represents mean and standard deviation of the ITRs associated with different SS-mVEP detectors across the 10 subjects. The DvCCA outperforms baselines in terms of speed of detection resulting in ITR of 21.5 ± 6.7 , 24.8 ± 5.5 , 35.2 ± 2.7 , and 33.3 ± 6.2 for the Radial-Zoom, Reciprocal Rotation, Swing and Sway paradigms, respectively. The Swing paradigm with DvCCA classifier has the best ITR performance. Through our comparisons, the proposed DvCCA shows superiority for classifying SSmVEP paradigms.

5.5 Summary

Given recent surge of interest on SSmVEP-based BCI systems, the chapter proposes a new deep learning based classifier, referred to as the Deep Video Canonical Correlation Analysis (DvCCA). The proposed DvCCA model consists of a Video Feature Extractor (VFE) layer that uses characteristics of videos to fit to the template EEG signals of each individual independently, which results in the extracted features to be more correlated with the stimulation video signal. The proposed VFE uses characteristics of videos eliminating problems associated with more complicated networks such as overfitting and/or lack of enough training data. The proposed DvCCA is evaluated based on a real EEG dataset outperforming its state-of-the-art counterpart and achieving accuracy of 80.1 ± 7.5 , 85.8 ± 4.7 , 96.8 ± 1.7 , 90.1 ± 7.1 over the four SSmVEPs.

Chapter 6

Summary and Future Research

Directions

This chapter concludes the thesis by providing a list of important contributions made throughout this dissertation. Furthermore, potential directions for future research are presented.

6.1 Summary of Thesis Contributions

Recent advancements in biomedical health technologies and the evolution of Artificial Intelligence (AI) coupled with advanced Electroencephalography (EEG) sensor technologies have paved the way for the further evolution of Brain-Computer Interface (BCI) systems. BCI systems have found several practical applications of significance ranging from rehabilitation/assistive systems to smart consumer technologies. Based on recent technology trends, it seems that leading technology companies are focused to couple BCI systems with Augmented Reality (AR) visors. In this regard, the thesis focused on development of advanced Machine Learning (ML) and Biological Signal Processing (BSP) methodologies for potential incorporation in AR-based BCI systems. In this context, Steady-State Visual Evoked Potentials (SSVEPs) targeting visual nerve pathways are considered as the main BCI technology for potential integration with AR due to their superior characteristics such as high accuracy and Information Transfer Rate (ITR). However, continuous utilization of SSVEPs causes eye fatigue and puts an excessive mental load on subjects. This mental load can be attributed

to the following key issues: (i) Eye fatigue with low-frequency flickering, and; (ii) Higher risk of induced epileptic seizure with medium-frequency flickering. To address these issues, Steady-State motion Visual Evoked Potentials (SSmVEPs) comprising of reversal periodic movements of different shapes are introduced as an attractive alternative. Although the SSmVEP-based BCIs induce less eye fatigue, their frequency detection accuracy and ITR are not comparable to that of the SSVEPs yet. To construct a robust and reliable SSmVEP-based BCI system, the thesis made the following three main contributions:

- (1) **Study on Novel Designs with Reduced Fatigue for Steady-State Motion Visual Evoked Potentials [61]:** The thesis proposed two novel Steady-State motion Visual Evoked Potential (SSmVEP) paradigms with low luminance contrast. The key issue targeted is the fatigue of flicker (or brightness modulation) via development of different patterns with oscillating expansion and contraction motions. The proposed flicker-free SSmVEP paradigms are designed and selected through an extensive set of experiments. The visual fatigue level is optimized during the testing experiments for the selected designs. As a result, one of the proposed paradigms even outperformed its SSVEP-based counterparts, which is a significant achievement. To the best of our knowledge, this is the first time that robust SSmVEP paradigms with reduced visual fatigue can provide better performance compared to SSVEPs. Furthermore, comparisons between complex SSmVEP paradigms are performed in terms of accuracy, ITR, and visual fatigue level.
- (2) **DF-SSmVEP: Dual Frequency Aggregated Steady-State Motion Visual Evoked Potential Design with Bifold Canonical Correlation Analysis [63]:** To address lower accuracy and ITR of SSmVEP designs, the thesis proposed an intuitively pleasing, novel, and innovative dual-frequency aggregated modulation paradigm. Referred to as the DF-SSmVEP, the proposed design is constructed by concurrently integrating “Radial Zoom” and “Rotation” motions in a single target without increasing the trial length. Additionally, the general theoretical framework is derived for development of such novel integrated SSmVEP paradigms. To this end, we generate the novel idea of coding to modulate two frequencies within a single

target. The proposed mechanism of integration can lead to a robust and quick SSmVEP-based system. Using the proposed integration technique, basic SSmVEP paradigms that are not individually applicable can become robust enough to be utilized in BCI systems after integration. Finally, a new spatial filtering approach, BCCA is developed. This specific unsupervised classification model outperforms regular CCA because of its high compatibility with the design of the DF-SSmVEP. The proposed DF-SSmVEP is evaluated via a real EEG dataset achieving the average ITR of 30.07 ± 1.97 and the average accuracy of 92.5 ± 2.04 .

- (3) **Deep Video Canonical Correlation Analysis for Steady-State motion Visual Evoked Potential Feature Extraction [62]:** The thesis proposed a new deep learning-based classifier, referred to as the Deep Video Canonical Correlation Analysis (DvCCA). This supervised model aims to address the vagueness issue of the deep learning approaches within the BCI context. The proposed DvCCA model consists of a Video Feature Extractor (VFE) layer that uses characteristics of videos to fit into the template EEG signals of each individual, independently. This results in the extracted features to be more correlated with the stimulation video signal. The proposed VFE uses features of videos eliminating problems associated with more complicated networks such as overfitting and/or lack of enough training data. According to the literature, one of the best frequency classifier used in SSmVEP-based BCIs are CNNs. The proposed DvCCA is evaluated based on a real EEG dataset outperforming its state-of-the-art CNN-based counterparts and achieving the accuracy of 80.1 ± 7.5 , 85.8 ± 4.7 , 96.8 ± 1.7 , 90.1 ± 7.1 over the four novel SSmVEP paradigms designed for this experiment. As another contribution, this is the first time that a model can directly discover connections between stimulation videos and EEG signals in visual BCIs. This can be the first step to solve the problem reversely and understand the connection between VEP's intensity and the stimuli' shape.

6.2 Future Research

- (1) **Analysis of Visual Fatigue:** In this thesis, the fatigue level for each paradigm is measured using the reduction in accuracy of consecutive sessions. Some features of EEG signals collected from the prefrontal cortex can be integrated into the main EEG samples to provide a further numerical comparison between paradigms in terms of fatigue level and mental load.
- (2) **Deploying Deep Reinforcement Learning to design VEP Paradigms:** Providing comfortable, convenient, user-friendly, and user-specific BCI platforms are crucial for incorporation of BCIs within AR systems. As stated in the thesis, alteration of each pixel's color across time can evoke the brain signals in the occipital part of the brain. The evoked signals of the stimulus's pixels superpose to develop SSmVEP within the brain signals. It is, however, impractical to test all possible pixel-colors since several trials are required to make sure that the extracted feedbacks are uncorrelated with the cocktail-party type noise of the brain signals. Moreover, choosing arbitrary colors for pixels does not necessarily generate motion of meaningful shapes. A fruitful direction for future research is to use a bank of SSmVEP paradigms to generate new, subject-specific, and meaningful shapes. Generated paradigms can be designed to be highly compatible with the neuro characteristics of a given subject to achieve the highest possible ITR and accuracy. Subject-specific and discriminative shapes can be designed using Generative Adversarial Networks (GAN) coupled with Convolutional Neural Network (CNN) based classifiers. Furthermore, we planned to replace the human designers, with reinforcement learning in our closed-loop system. To this end, we can leverage deep Reinforcement Learning (RL) to construct motion videos evoking SSmVEPs, via optimal alteration of the primary paradigms based on the reward given by EEG signals. More specifically, the gradient of the video modifier is chosen in such a way that the reward function (accuracy of the CNN classification) gets maximized to enhance the Signal to Noise Ratio (SNR), i.e., the envisioned deep model learns the important pixels with regards to achievable SNR via an RL approach. The envisioned model, accordingly, changes the pixels, which have a high impact on the SNR in such a way that the modified shapes are still recognizable. This envisioned future research project is believed to be significant for future adoption of

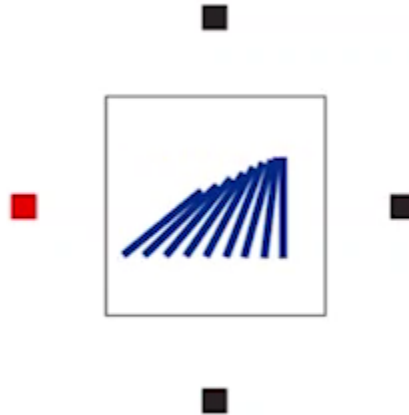


Figure 6.1: A sample of the designed MVEP paradigm.

AI, and AR within BCI technologies to provide an alternative communication medium for development and advancement in this domain.

- (3) **Understanding the Relationship between Video pixels and EEG Signals:** The deep learning-based algorithm reported in this thesis is supervised, and it is fed with the videos of the paradigm directly. This model is designed based on averaging signals derived from the paradigm's video. The weights are intensified as we get farther from the center of attention where the subject is asked to stare. Although a linear combination of pixels' signals based on eccentricity does not work properly, one susceptible direction is to understand the complex relationship between the harmonics of EEG evoked by the videos and the importance of the pixels. An unsupervised model can then be designed for the frequency detection task so that the dynamics of the visual pathways are modeled completely in this model. Additionally, one of the major problems that affect the performance of SSVEPs is signal interference. In other words, the impact of other targets can distort the main target signal. Using a general model, we can estimate other targets' signal interference to filter the superposed signal so that better performance is achieved.
- (4) **Developing an Unsupervised Classifier for a General Form of Motion-onset Visual Evoked Potentials (MVEPs):** As mentioned in the thesis, Motion-Onset Visual Evoked Potentials

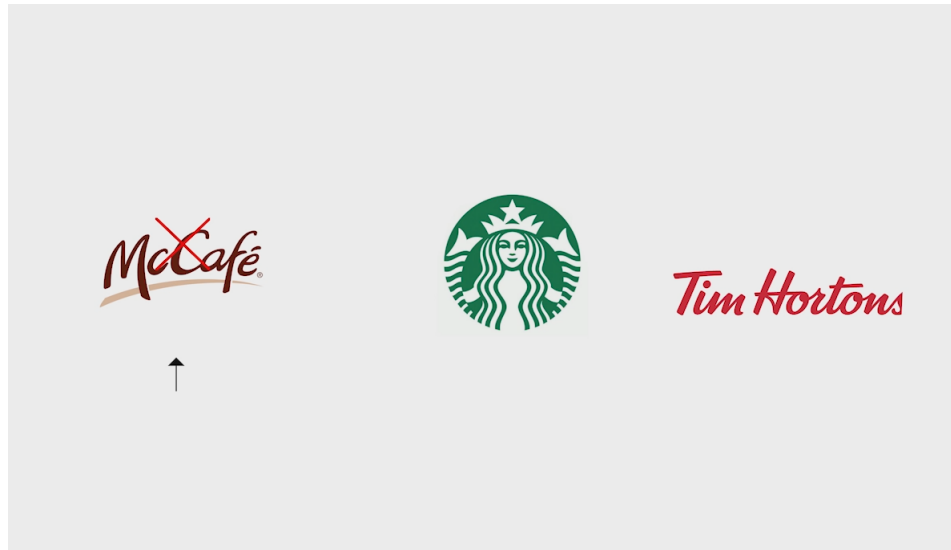


Figure 6.2: A sample of the designed paradigm where logos of specific companies are inserted oscillating with the same frequency.

(mVEPs) [41, 57, 58], which elicit $P1$, $N2$, and $P2$ components in EEG signal, are introduced as attractive alternatives to SSVEPs. However, the shortage of low accuracy and ITR applies to these paradigms as well. Moreover, targets within an MVEP do not necessarily possess orthogonal base-frequencies, therefore, it is impossible to demodulate EEG signals to identify the target. To classify targets, a supervised algorithm using an ERP component is utilized. These techniques segment the EEG signals into time windows with a length of 300 to 400 milliseconds. The segments, which are short time series, represent the features of MVEPs. Most of the existing approaches use the correlation between segments of test and train samples without extracting any extra features from the frequency spectrum of the signals. We have also designed some MVEP paradigms, including a single-stimulus and multitarget around it as shown in Fig. 6.1. Our main goal was to draw a fixed pattern in the frequency spectrum of the signals based on the corresponding target's location. Hence, as we guess the reference signal of the MVEP, we can feed the EEG signal into CCA-based classifiers. However, due to the high volume of noise, there was no record of significant results in our initial experiment. This is a fruitful direction for further research.

- (5) **Using the Same Frequency for Different Shapes in BCI:** Another SSmVEP-based paradigm that is worth investigating is the one that has the same frequency, however different shapes,

in its targets. For instance, as shown in Fig. 6.2, two logos of specific companies are inserted oscillating with the same frequency in our stimulation videos. Then, the subject stares at logos separately in different trials. The main goal is to realize which logo is focused on in each trial by only processing EEG signals. The amplitudes of the harmonics of the modulated frequency varied across two classes. The targets were then classified using the ratio of the harmonics. However, the accuracy of the system was not enough to be utilized in real BCIs. Moreover, existing unsupervised classifiers such as CCA, are weak to classify targets based on the ratio of the harmonics in the signal's spectrum. In that sense, there is a potential to introduce an inductive unsupervised model.

Bibliography

- [1] M.L. Gill, *et al.* “Neuromodulation of Lumbosacral Spinal Networks Enables Independent Stepping After Complete Paraplegia,” *Nature Medicine*, Sep. 2018.
- [2] C.A. Angeli, *et al.*, “Recovery of Over-Ground Walking after Chronic Motor Complete Spinal Cord Injury,” *New Engl. J. Med.*, vol. 379, pp. 1244-1250, Sep. 2018.
- [3] R.P.N. Rao and R. Scherer, “Brain-Computer Interfacing [In the Spotlight],” *IEEE Signal Processing Magazine*, vol. 27, no. 4, pp. 152-150, July 2010.
- [4] J. R. Wolpaw, and E. W. Wolpaw, “Brain-Computer Interfaces. Principles and Practice,” *New York, NY, USA: Oxford Univ. Press*, 2012.
- [5] L.V. Dokkum, T. Ward, I. Laffont, “Brain Computer Interfaces for Neurorehabilitation: Its Current Status as a Rehabilitation Strategy,” *Annals Physical & Rehabil. Medicine*, vol. 58, no. 1, pp. 3-8, 2015.
- [6] O. Talakoub, C. Marquez-Chin, M.R. Popovic, J. Navarro, E.T. Fonoff, C., Hamani, and W. Wong, “Reconstruction of Reaching Movement Trajectories using Electrographic Signals in Humans,” *PLoS ONE*, vol. 12, no. 9, 2017.
- [7] S. Shahtalebi, and A. Mohammadi, “Bayesian Optimized Spectral Filters Coupled with Ternary ECOC for Single Trial EEG Classification,” *IEEE Trans. Neural Syst. Rehabil. Eng.*, 2018.
- [8] G. Kalantar, M. Mirgholami, A. Asif and A. Mohammadi, “Improving the Performance of Motor Imagery EEG-based BCIs via an Adaptive Epoch Trimming Mechanism,” *IEEE Global Con. Signal & Inf. Process. (GlobalSIP)*, pp. 479-483, 2018.
- [9] H. Huang *et al.*, “An EEG-Based Brain Computer Interface for Emotion Recognition and Its Application in Patients with Disorder of Consciousness,” *IEEE Trans. Affective Computing*, 2019.

- [10] H. Si-Mohammed *et al.*, “Towards BCI-based Interfaces for Augmented Reality: Feasibility, Design and Evaluation,” *IEEE Trans. Visualization and Computer Graphics*, 2019. In Press.
- [11] L. Angrisani, P. Arpaia, D. Casinelli and N. Moccaldi, “A Single-Channel SSVEP-Based Instrument With Off-the-Shelf Components for Trainingless Brain-Computer Interfaces,” *IEEE Trans. Instrumentation and Measurement*, 2019. In Press.
- [12] F. Carrino, J. Dumoulin, E. Mugellini, O.A. Khaled, and R. Ingold, “A Self-paced BCI System to Control an Electric Wheelchair: Evaluation of a Commercial, Low-cost EEG Device,” *IEEE Biosignals and Biorobotics Conference (BRC)*, pp. 1-6, 2012.
- [13] T. Kaufmann, A. Herweg, and A. Kübler, “Toward Brain-computer Interface based Wheelchair Control Utilizing Tactually-Evoked Event-Related Potentials,” *J. Neuro. & Rehab.*, vol. 11, no. 1, 2014.
- [14] R. Leeb, L. Tonin, M. Rohm, L. Desideri, T. Carlson, J.D.R. Millán, “Towards Independence: A BCI Telepresence Robot for People with Severe Motor Disabilities,” *Proc. IEEE*, vol. 103, no. 6, pp. 969-982, 2015.
- [15] A. Vempaty, B. Kailkhura, P.K. Varshney, “Human-Machine Inference Networks For Smart Decision Making: Opportunities and Challenges,” <https://arxiv.org/abs/1801.09626>, 2018.
- [16] B. Kerous, F. Skola, and F. Liarokapis, “EEG-based BCI and Video Games: A Progress Report,” *Virtual Reality*, vol. 22, pp. 119-135, 2018.
- [17] P. Stawicki *et al.*, “Investigating Spatial Awareness within an SSVEP-based BCI in Virtual Reality,” *IEEE International Conference on Systems, Man, and Cybernetics (SMC)*, pp. 615-618, 2018.
- [18] W. Yan *et al.*, “Steady-State Motion Visual Evoked Potential (SSMVEP) based on Equal Luminance Colored Enhancement,” *PLoS One*, vol. 12, no. 1, pp. 1-18, 2017.
- [19] J.J. Podmore, T.P. Breckon, N.K.N. Aznan, J.D. Connolly, “On the Relative Contribution of Deep Convolutional Neural Networks for SSVEP-Based Bio-Signal Decoding in BCI Speller Applications,” *IEEE Trans. Neural Syst. Rehabil. Eng.*, vol. 27, no. 4, pp. 611-618, April 2019.
- [20] E.K. Kalunga *et al.*, “Online SSVEP-based BCI using Riemannian Geometry,” *Neurocomputing*, vol. 191, pp. 55-68, May 2016.

- [21] C. Han, G. Xu, J. Xie, C. Chen, S. Zhang, “Highly Interactive Brain–Computer Interface Based on Flicker-Free Steady-State Motion Visual Evoked Potential,” *Nature Scientific Reports*, vol. 8, 2018.
- [22] G. Bin, X. Gao, Y. Wang, B. Hong and S. Gao, “VEP-based Brain-Computer Interfaces: Time, Frequency, and Code Modulations,” *IEEE Computational Intelligence Magazine*, vol. 4, no. 4, pp. 22-26, 2009.
- [23] J. Xie, G. Xu, J. Wang, F. Zhang, Y. Zhang “Steady-State Motion Visual Evoked Potentials Produced by Oscillating Newton’s Rings: Implications for Brain-Computer Interfaces,” *PLoS ONE*, vol. 7, no. 6, 2012.
- [24] P. Afshar, A. Mohammadi and K. N. Plataniotis, “Brain Tumor Type Classification via Capsule Networks,” *IEEE Int. Conference on Image Processing (ICIP)*, pp. 3129-3133, 2018.
- [25] F. Lotte *et al.*, “A Review of Classification Algorithms for EEG-based Brain-Computer Interfaces: A 10 Year Update,” *J. Neural Eng.*, vol. 15, no. 3, 2018.
- [26] B.Z. Allison, E.W. Wolpaw, and J.R. Wolpaw, “Brain-Computer Interface Systems: Progress and Prospects,” *Expert Review of Medical Devices*, vol. 4, no. 4, pp. 463-474, 2007.
- [27] W. Yan *et al.*, “Steady-State Motion Visual Evoked Potential (SSMVEP) based on Equal Luminance Colored Enhancement,” *PLoS One*, vol. 12, no. 1, pp. 1-18, 2017.
- [28] X. Chai, Z. Zhang, K. Guan, G. Liu, N. Niu, “A Radial Zoom Motion-Based Paradigm for Steady State Motion Visual Evoked Potentials,” *Frontiers in Human Neuroscience*, vol. 13, 2019.
- [29] M. Wang *et al.*, “A New Hybrid BCI Paradigm based on P300 and SSVEP,” *J. Neuroscience Methods*, vol. 244, pp. 16-25, 2015.
- [30] X. Chen, *et al.*, “Removal of Muscle Artifacts From the EEG: A Review and Recommendations,” *IEEE Sensors Journal*, vol. 19, no. 14, pp. 5353-5368, 2019.
- [31] S. Shahtalebi and A. Mohammadi, “Bayesian Optimized Spectral Filters Coupled With Ternary ECOC for Single-Trial EEG Classification,” *IEEE Trans. Neural Syst. Rehabil. Eng.*, vol. 26, no. 12, pp. 2249-2259, 2018.
- [32] K. Samanta, S. Chatterjee, and R. Bose, “Cross-Subject Motor Imagery Tasks EEG Signal Classification Employing Multiplex Weighted Visibility Graph and Deep Feature Extraction,” *IEEE Sensors Letters*, vol. 4, no. 1, pp. 1-4, 2020.

- [33] E. Dagois, A. Khalaf, E. Sejdic and M. Akcakaya, “Transfer Learning for a Multimodal Hybrid EEG-ftCD Brain-Computer Interface,” *IEEE Sensors Letters*, vol. 3, no. 1, pp. 1-4, 2019.
- [34] Y. Zhang, *et al.*, “Hierarchical Feature Fusion Framework for Frequency Recognition in SSVEP-based BCIs,” *Neural Networks*, vol. 119, pp. 1–9, 2019.
- [35] Y. Kimura, T. Tanaka, H. Higashi, N. Morikawa, “SSVEP-based Brain-Computer Interfaces using FSK-Modulated Visual Stimuli,” *IEEE Trans. Biomed. Eng.*, vol. 60, no. 10, pp. 2831-2838, 2013.
- [36] X. Zhao, D. Zhao, X. Wang, X. Hou, “A SSVEP Stimuli Encoding Method Using Trinary Frequency-shift Keying Encoded SSVEP (TFSK-SSVEP),” *Frontiers in Human Neuroscience*, vol. 11, 2017.
- [37] Q. Wei, S. Feng, Z. Lu, “Stimulus Specificity of Brain-Computer Interfaces based on Code Modulation Visual Evoked Potentials,” *PloS One*, vol. 11, no. 5, 2016.
- [38] M. Nakanishi, *et al.*, “A High-Speed Brain Speller using Steady-State Visual Evoked Potentials,” *Int. J. Neural Systems*, vol. 24, no. 06, 2014.
- [39] Y. Zhang, *et al.*, “Multiple Frequencies Sequential Coding for SSVEP-based Brain-Computer Interface,” *PloS One*, vol. 7, no. 3, 2012.
- [40] B. Kadioglu, I. Yildiz, P. Closas, M. B. Fried-Oken and D. Erdogmus, “Robust Fusion of c-VEP and Gaze,” *IEEE Sensors Letters*, vol. 3, no. 1, pp. 1-4, 2019.
- [41] R. Beveridge, S. Wilson, M Callaghan, D. Coyle, “Neurogaming with Motion-onset Visual Evoked Potentials (MVEPs): Adults versus Teenagers,” *IEEE Trans. Neural Syst. Rehabil. Eng.*, vol. 27, no. 4, pp. 572-581, 2019.
- [42] W. Yan, G. Xu, L. Chen, and X. Zheng, “Steady-state Motion Visual Evoked Potential (SSmVEP) Enhancement Method based on Time-Frequency Image Fusion,” *Computational Intelligence and Neuroscience*, 2019.
- [43] C. Han, G. Xu, J. Xie, C. Chen, S. Zhang, “Highly Interactive Brain-Computer Interface based on Flicker-Free Steady-State Motion Visual Evoked Potential,” *Nature Scientific Reports*, vol. 8, no. 1, 2018.
- [44] W. Yan, *et al.*, “Four Novel Motion Paradigms based on Steady-state Motion Visual Evoked Potential,” *IEEE Trans. Biomed. Eng.*, pp. 1696–1704, Aug. 2018.

- [45] M. Nakanishi , Y. Wang, Y. Mitsukura, T.P. Jung, “An Approximation Approach for Rendering Visual Flickers in SSVEP-based BCI using Monitor Refresh Rate,” *IEEE Int. Con. Eng. Medicine & Biology Society (EMBC)*, pp. 2176–2179, 2013.
- [46] J. Xie, G. Xu, J. Wang, F. Zhang, and Y. Zhang, “Steady-state Motion Visual Evoked Potentials Produced by Oscillating Newton’s Rings: Implications for Brain-computer Interfaces,” *Plos one*, vol. 7, no. 6, pp. e39707, 2012.
- [47] <https://github.com/raykakarimi/DF-SSmVEP-videos>
- [48] g.Nautilus. (2018). g.tech: g.nautilus wireless biosignal acquisition, <http://www.gtec.at/products/hardware-and-accessories/g.nautilus-specs-feature>.
- [49] M. Mirgholami, S. Shahtalebi, W. Cui, R. Karimi, A. Asif, and A. Mohammadi, “Adaptive Subject-specific Bayesian Spectral Filtering for Single Trial EEG Classification,” *IEEE Global Conference on Signal and Information Processing (GlobalSIP)*, pp. 1-5, 2019.
- [50] G. Schalk, *et al.*, “BCI2000: A General-Purpose Brain-Computer Interface (BCI) System,” *IEEE Trans. Biomedical Eng.*, vol. 51, no. 6, pp. 1034-1043, 2004.
- [51] L.I. Jovanovic, N. Kapadia, L. Lo, V. Zivanovic, M.R. Popovic, C. Marquez-Chin “Restoration of Upper Limb Function After Chronic Severe Hemiplegia: A Case Report on the Feasibility of a Brain-Computer Interface-Triggered Functional Electrical Stimulation Therapy,” *American J. Physical Medicine & Rehabilitation*, vol. 99, 2020.
- [52] U. Chaudhary, N. Birbaumer, and A. Ramos-Murguialday, “Brain-Computer Interfaces for Communication and Rehabilitation,” *Nature Reviews Neurology*, vol. 12, no. 9, 2016.
- [53] Q. Jiang, F. Shao, W. Lin, and G. Jiang, “On Predicting Visual Comfort of Stereoscopic Images: A Learning to Rank based Approach,” *IEEE Signal Process. Lett.*, vol. 23, vol. 2, pp. 302-306, 2016.
- [54] E.K. Kalunga, S. Chevallier, and Q. Barthélemy, “Transfer Learning for SSVEP-based BCI using Riemannian Similarities Between Users,” *European Signal Process. Con. (EUSIPCO)*, pp. 1685-1689, 2018.
- [55] E. Kinney-Lang, A. Ebied, and J. Escudero, “Building a Tensor Framework for the Analysis and Classification of Steady-state Visual Evoked Potentials in Children,” *European Signal Processing Conference (EUSIPCO)*, pp. 296-300, 2018.

- [56] J. Xie, *et al.*, “Effects of Mental Load and Fatigue on Steady-state Evoked Potential based Brain Computer Interface Tasks: A Comparison of Periodic Flickering and Motion-reversal based Visual Attention,” *PloS one*, vol. 11, no. 9, 2016.
- [57] J. Chen, *et al.*, “A Single-stimulus, Multitarget BCI based on Retinotopic Mapping of Motion-onset VEPs,” *IEEE Trans. Biomedical Eng.*, vol. 66, no. 2, pp. 464-470, 2018.
- [58] T. Ma, *et al.*, “The Extraction of Motion-onset VEP BCI Features based on Deep Learning and Compressed Sensing,” *J. Neuroscience Methods*, vol. 275, pp. 80-92, 2017.
- [59] C. Han, G. Xu, J. Xie, C. Chen, and S. Zhang, “Highly Interactive Brain–Computer Interface based on Flicker-Free Steady-state Motion Visual Evoked Potential,” *Scientific Reports*, vol. 8, no. 1, 2018.
- [60] F. Sobreira, C. Tremmel, and D. J. Krusienski, “Modeling the Visual Pathway for Stimulus Optimization in Brain-Computer Interfaces,” *European Signal Processing Conference (EUSIPCO)*, pp. 1672-1675, 2018.
- [61] R. Karimi, L. Rosero, M. Nirgholami, A. Asif, and A. Mohammadi, “Study on Novel designs with Reduced Fatigue for Steady State Motion Visual Evoked Potentials,” *IEEE Global Conference on Signal and Information Processing (GlobalSIP)*, pp 1-5, 2019.
- [62] R. Karimi, L. Rosero, Amir Asif, and A. Mohammadi, “Deep Video Canonical Correlation Analysis for Steady State motion Visual Evoked Potential Feature Extraction,” *European Signal Processing Conference (EUSIPCO)*, 2020.
- [63] R. Karimi, A. Mohammadi, Amir Asif, H. Benali, “DF-SSmVEP: Dual Frequency Aggregated Steady-State Motion Visual Evoked Potential Design with Bifold Canonical Correlation Analysis,” Minor Revisions Requested at *IEEE Sensors Letter*, Oct. 2020.
- [64] W. Yan, *et al.*, “Study on the Effects of Brightness Contrast on Steady-state Motion Visual Evoked Potential,” *IEEE Int. Con. Eng. Medicine and Biology Society (EMBC)*, pp 2263-2266, 2017.
- [65] Z. Lin, C. Zhang, W. Wu, and X. Gao, “Frequency Recognition based on Canonical Correlation Analysis for SSVEP-based BCIs,” *IEEE Trans. Biomedical Eng.*, vol. 53, no. 12, pp. 2610-2614, 2006.
- [66] Y. Zhang, *et al.*, “Two-stage Frequency Recognition Method based on Correlated Component Analysis for SSVEP-based BCI,” *IEEE Trans. Neural Syst. Rehabil. Eng.*, vol. 26, no. 7, pp. 1314-1323, 2018.

- [67] M. Nakanishi, , *et al.*, “Enhancing Detection of SSVEPs for a High-speed Brain Speller using Task-related Component Analysis,” *IEEE Trans. Biomedical Eng.*, vol. 65, no. 1, pp. 104-112, 2017.
- [68] Z..M Zhang and Z.D. Deng, “A Kernel Canonical Correlation Analysis based Idle-state Detection Method for SSVEP-based Brain-Computer Interfaces,” *Advanced Materials Research*, vol. 341, pp. 634-640, 2012.
- [69] H. Vu, B. Koo, and S. Choi, “Frequency Detection for SSVEP-based BCI using Deep Canonical Correlation Analysis,” *IEEE Int. Con. Systems, Man, & Cybernetics (SMC)*, pp. 1983-1987, 2016.
- [70] Q. Liu, *et al.*, “Efficient Representations of EEG Signals for SSVEP Frequency Recognition based on Deep Multiset CCA,” *Neurocomputing*, vol. 378, pp. 36-44, 2020.
- [71] Z.K. Gao, *et al.*, Multivariate Weighted Recurrent Network for Analyzing SSmVEP Signals from EEG Literate and Illiterate,” *Europhysics Letters*, vol. 127, no. 4, 2019.
- [72] N. Khadijah, *et al.*, “On the Classification of SSVEP-based Dry-EEG Signals via Convolutional Neural Networks,” *IEEE Int. Con. Systems, Man, & Cybernetics (SMC)*, pp. 3726-3731, 2018.
- [73] T.H. Nguyen and W.Y. Chung, “A Single-Channel SSVEP-based BCI Speller using Deep Learning,” *IEEE Access*, vol. 7, pp. 1752-1763, 2018.
- [74] A. Ravi, N. Heydari Beni, J. Manuel, and N. Jiang, “Comparing User-dependent and User-independent Training of CNN for SSVEP BCI,” *J. Neural Engineering*, 2020.
- [75] G. Andrew, R. Arora, J. Bilmes, and K. Livescu, “Deep Canonical Correlation Analysis,” *International Conference on Machine Learning*, pp. 1247-1255, 2013.
- [76] M. Nakanishi, Y. Wang, Y.T. Wang, Y. Mitsukura, and T.P. Jung, “Generating Visual Flickers for Eliciting Robust Steady-state Visual Evoked Potentials at Flexible Frequencies using Monitor Refresh Rate,” *PloS one*, vol. 9, no. 6, 2014.
- [77] F. Kheiralla, M. Elmusharaf, “Simulated Biological Systems on the Information Systems,” *International Journal of Innovations & Advancement in Computer Science*, 2017.
- [78] I. Käthner, A. Kübler, S. Halder, “Rapid P300 brain-computer interface communication with a head-mounted display,” *Frontiers in Neuroscience*, vol. 9, 2015.
- [79] A. Beres, “Time is of the essence: A review of electroencephalography (EEG) and event-related brain potentials (ERPs) in language research,” *Springer*, vol. 42, 2017.

- [80] G. Henriksen, B. Kaada, “The Norwegian EEG society: University of Oslo September 8th, 1952 and November 4, 1952,” *Elsevier*, vol. 5, no. 1, 1953.
- [81] D. Wu, J. King, C. Chuang, C. Lin, T. Jung, “Spatial filtering for EEG-based regression problems in brain–computer interface (BCI),” *IEEE Transactions on Fuzzy Systems*, vol. 26, no. 2, 2017.